Gondwana Research 36 (2016) 488–502

Contents lists available at ScienceDirect

Gondwana Research

journal homepage: www.elsevier.com/locate/gr

Where was the Ailaoshan Ocean and when did it open: A perspective based on detrital zircon U–Pb age and Hf isotope evidence

Xiaoping Xia [a,*], Xiaosong Nie [a,b], Chun-Kit Lai [c], Yuejun Wang [d], Xiaoping Long [a], Sebastien Meffre [e]

[a] State Key Laboratory of Isotope Geochemistry, Guangzhou Institute of Geochemistry, Chinese Academy of Sciences, Wushan, Guangzhou, 510460, China
[b] University of Chinese Academy of Sciences, Beijing 100049, China
[c] Cenozoic Geoscience Editing, Hobart, TAS, 7005, Australia
[d] Department of Earth Sciences, Sun Yat-sen University, West Xinggang Road 135, Guangzhou, 510275, China
[e] Centre of Excellence in Ore Deposits (CODES), University of Tasmania, TAS 7005, Australia

ARTICLE INFO

Article history:
Received 20 November 2014
Received in revised form 31 July 2015
Accepted 7 August 2015
Available online 8 September 2015

Handling Editor: Y.P. Dong

Keywords:
Detrital zircon
U–Pb age and Hf isotope
Ailaoshan Belt
Paleo-Tethys
Yangtze/Indochina–Simao suture

ABSTRACT

The Indochina–Simao and Yangtze blocks were separated by a branch of the Paleo-Tethys Ocean, commonly referred as the Ailaoshan Ocean in the Paleozoic. Remnants of this Ailaoshan Ocean have been variably suggested to locate along (from east to west) the Ailaoshan fault, Jiujia–Anding fault and Amojiang–Lixianjiang fault. In order to test these models, we have carried out comprehensive detrital zircon U–Pb dating and Hf isotope analyses on the Cambrian to Devonian sedimentary units in the Ailaoshan Belt and its adjacent western margin of the Yangtze Block. Our results indicate marked detrital zircon provenance variation on different sides of the Ailaoshan–Tengtiaohe fault: detrital zircons from east of the fault display a diagnostic age peak at 730–900 Ma, which is characterized by both positive and negative $\varepsilon Hf(t)$ values with a Hf model age (T_{DM}^{C}) peak at ~1.8 Ga, whereas detrital zircons from west of the fault display two major age populations of 400–500 and 900–1000 Ma, both characterized by mainly negative $\varepsilon Hf(t)$ values with a Hf model age (T_{DM}^{C}) peak at ~2.1 Ga. Our new data indicate that detritus from east and west of the Ailaoshan–Tengtiaohe fault may have been mainly derived from, respectively, the Yangtze Block and Indochina–Simao blocks, thus suggesting the fault may represent the actual suture between the two blocks. Our study also reveals that the Ailaoshan Ocean may have started its early continental rift in the Early Silurian.

1. Introduction

The modern Southeast (SE) Asia was formed during the Phanerozoic by a series of complex collision and accretion processes of many allochthonous continental blocks such as South China (including Yangtze and Cathaysia), Indochina–Simao, Sibumasu and other micro-continental fragments and slivers (Fig. 1) (Metcalfe, 2006; Faure et al., 2014). These blocks are usually regarded to have been derived from the northwestern Gondwana margin as three successive strips of continental blocks separated during the Paleozoic to Early Mesozoic. These blocks then travelled north to amalgamate progressively during the Late Paleozoic to Cenozoic along the southern Eurasia margin (Metcalfe, 1996, 2002; Rogers and Santosh, 2003; Metcalfe, 2006, 2011, 2013; Q.F. Wang et al., 2014; Zaw et al., 2014). This has resulted in the consecutive opening and closure of three Tethyan oceans, namely the Paleo-Tethys, Meso-Tethys and Neo-Tethys (Rogers and Santosh, 2003; Metcalfe, 2011, 2013), among which the Paleo-Tethys is the most enigmatic.

Previous studies suggested two Paleo-Tethyan branches in SE Asia, namely the Main Paleo-Tethys represented by the Changning–Menglian–Inthanon suture (Hara et al., 2012; Kamata et al., 2012), and the Ailaoshan Ocean represented by the Jingshajiang–Ailaoshan suture (Sone and Metcalfe, 2008; Zaw et al., 2014). It has been commonly accepted that the Main Paleo-Tethys had opened in the Silurian–Devonian and closed in the Triassic by an east-directed (modern orientation) subduction beneath Indochina–Simao (Metcalfe, 2013; Zaw et al., 2014). As for the Ailaoshan Ocean, structural overprinting and displacement related to the Cenozoic indentation tectonics of SE Asia (Tapponnier et al., 1990; Leloup et al., 2007; Lin et al., 2012) have led to several unresolved issues: the first issue centers on when and how the Ailaoshan Ocean was opened. Based on fossil evidence and zircon U–Pb dating of volcanic rocks, some researchers suggested that the ocean may have opened by back-arc spreading related to north-directed subduction of the Main Paleo-Tethys beneath Indochina–Simao in the Late Devonian–Early Carboniferous or Permian (Wang et al., 2000; Metcalfe, 2002; Metcalfe, 2006; Fan et al., 2010; Pan et al., 2012). However, other researchers considered it as an Atlantic-type ocean which underwent a complete plate tectonic cycle (continental rift – middle ocean ridge spreading – continental collision) from the Silurian–Devonian to

* Corresponding author. Tel.: +86 20 85290392.
E-mail address: xpxia@gig.ac.cn (X. Xia).

http://dx.doi.org/10.1016/j.gr.2015.08.006
1342-937X/

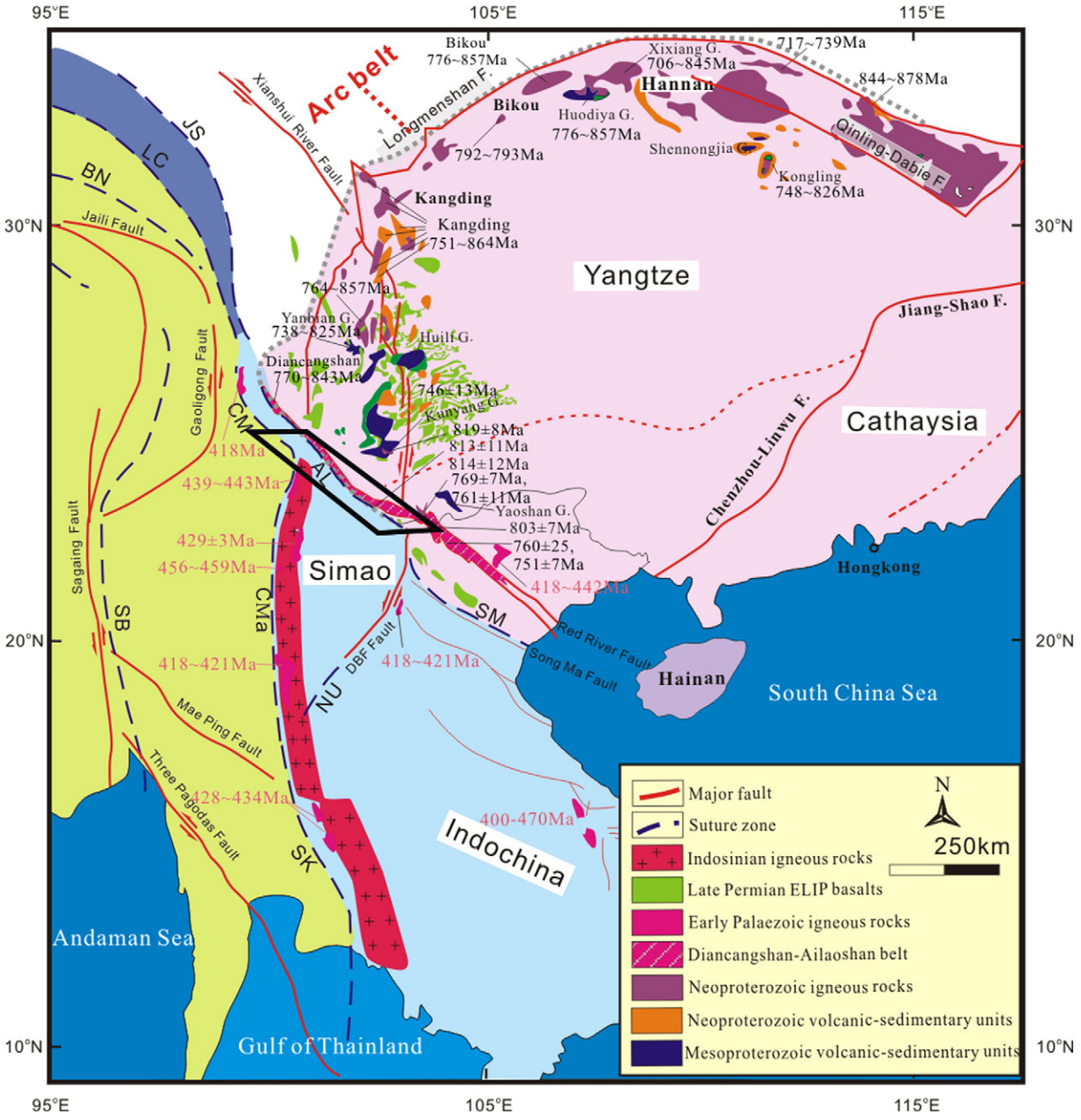

Fig. 1. Tectonic outline of SE Asia (modified after Cai et al. (2014)). Abbreviations: SM, Song Ma; AL, Ailaoshan; JS, Jinshajiang; LC, Langcangjiang; CM, Changling–Menglian; CMa, Chiang Mai; SK, Sra Kaeo; NU, Nan–Uttaradit; BN, Bangong–Nujiang; SB, Shan Boundary.

Triassic (Zhong et al., 1998; Jian et al., 2009a,b; Zi et al., 2012, 2013; Lai et al., 2014a,b). The second issue relates to the exact location of the Yangtze/Indochina–Simao suture. Possible suture locations have been variably suggested to be (from east to west) the Ailaoshan fault (Sone and Metcalfe, 2008), the Jiujia–Anding fault (Q.F. Wang et al., 2014) and the Amojiang–Lixianjiang fault (Chung et al., 1997) (Fig. 2).

To constrain the opening time of the Ailaoshan Ocean and delineate the suture between Yangtze and Indochina–Simao, we have carried out comprehensive detrital zircon U–Pb dating and Hf isotope analyses on the Cambrian to Devonian sedimentary units in the Ailaoshan Belt and its adjacent western Yangtze margin. Our results indicate distinctive detrital provenance variations for samples collected from different parts of the belt, which can be used to delineate the boundary location. Our data also provide new clues on the Paleozoic tectonic settings of the Ailaoshan Belt.

2. Geological settings and sampling

2.1. Overview

The Ailaoshan Belt in SW Yunnan, China (Fig. 1., >300 km long and ca. 20–100 km wide) is located between the Yangtze and the Indochina–Simao blocks. It is bounded by the Amojiang–Lixianjiang fault to the west and the Red River fault to the east (Fig. 2) (YNGMR, 1990; Xiong et al., 1998). The Ailaoshan Belt continues to the Jinshajiang Belt to the northwest (Mo et al., 1998; Zhong et al., 1998; Wang et al., 2000), whereas its southeast extension is largely uncertain and various geological terranes in northern Vietnam/Laos have been proposed (Findlay, 1997; Lepvrier et al., 2008). Strike-slip deformation associated with the Cenozoic India–Asia collision has tectonically reactivated the Ailaoshan Belt along a series of faults, e.g., the Red River, Ailaoshan, Jiujia–Anding and Amojiang–Lixiangjiang and Tengtiaohe

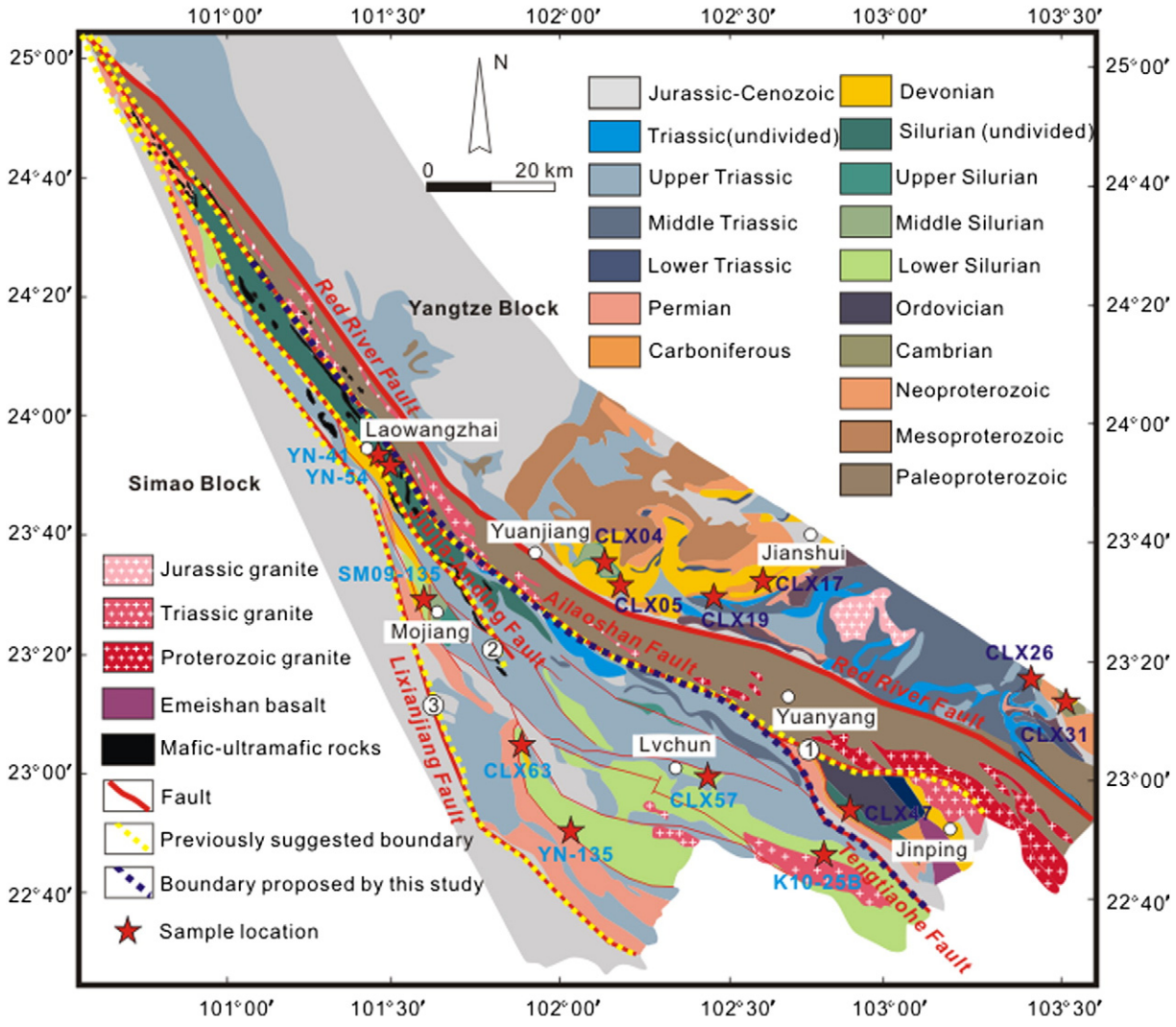

Fig. 2. Geological map of the Ailaoshan Belt. This figure is cited from Fig. 2 by Q.F. Wang et al. (2014) with addition of sample locations and possible locations of the Yangtze/Indochina–Simao suture. Yellow dotted lines with numbers 1, 2 and 3 are the possible suture locations proposed by Sone and Metcalfe (2008), Chung et al. (1997), Q.F. Wang et al. (2014), respectively.

faults (Tapponnier et al., 1990; Leloup et al., 2007; Searle et al., 2010). Among these faults, the Ailaoshan has divided the Ailaoshan belt into two major lithotectonic successions (Fig. 2): to the northeast of the fault, there are high-grade metamorphic rocks, also known as the Precambrian Ailaoshan Complex (YNGMR, 1990), whereas to the southwest there are greenschist facies-metamorphosed Silurian to Triassic volcanic–sedimentary strata and ultramafic–felsic intrusions (YNGMR, 1990; Zhong et al., 1998; X. Li, 2003; Fan et al., 2010).

The Yangtze Block (Figs. 1 and 2) comprises Archean to Paleoproterozoic crystalline basement and Neoproterozoic to Upper Paleozoic marine carbonates and terrigenous clastic rocks (Qiu et al., 2000; Zhao and Cawood, 2012; B.D. Wang et al., 2013; Cawood et al., 2013; Y. Wang et al., 2013). Neoproterozoic low-grade meta-terrigenous clastic rocks and volcanic–siliciclastic interbeds are widespread along the western Yangtze margin. A Neoproterozoic magmatic and metamorphic belt extends from Hannan (Shanxi Province) through Kangding (Sichuan Province) to Yuanjiang (Yunnan Province) (Fig. 1) (Li et al., 2002; Zhou et al., 2002a; Z. Li, 2003; Zhou et al., 2006; Wang et al., 2011; Cai et al., 2014; Qi et al., 2012, 2014). This belt has recently been suggested as a Neoproterozoic arc (i.e., Hannan–Panxi–Yuanjiang arc), comprising Neoproterozoic (Tonian to Cryogenian; 880–720 Ma) arc-related igneous rocks (Zhou et al., 2002b, 2006; Sun et al., 2008, 2009). Western Yangtze Block had experienced another episode of intense magmatism during the emplacement of the Late Permian (~260 Ma) Emeishan Large Igneous Province (ELIP) (Chung and Jahn, 1995; Shellnutt and Zhou, 2007; Shellnutt et al., 2008; Xu et al., 2008).

Between the Ailaoshan Belt and the Changning–Menglian suture zone is the Simao Block (Wu et al., 1995), which represents the northern continuation of the Indochina Block (Metcalfe, 1996, 2013). The Simao Block is largely covered by Mesozoic and Cenozoic red beds. Paleozoic sedimentary rocks and metamorphic basement including Damenglong and Chongshan complexes are only locally exposed on the western edge of the block (Wu et al., 1995; Zhong et al., 1998; Wang et al., 2000). An extensive Permo-Triassic mafic to felsic volcanic sequence is distributed along the Lancang–Mekong River on the western Simao margin. Ordovician–Silurian igneous rocks have been reported on the western margin of the Indochina–Simao Block (Khositanont et al., 2008; Mao et al., 2012; Lehmann et al., 2013; B.D. Wang et al., 2013; Nie et al., 2015), which are interpreted as a subduction-related arc (Khositanont et al., 2008; Nie et al., 2015).

2.2. Stratigraphic sections and samples

The stratigraphic sections of the Ailaoshan belt can be summarized into two types: the Mojiang–Lvchun type and the Jinping type (Fig. 3).

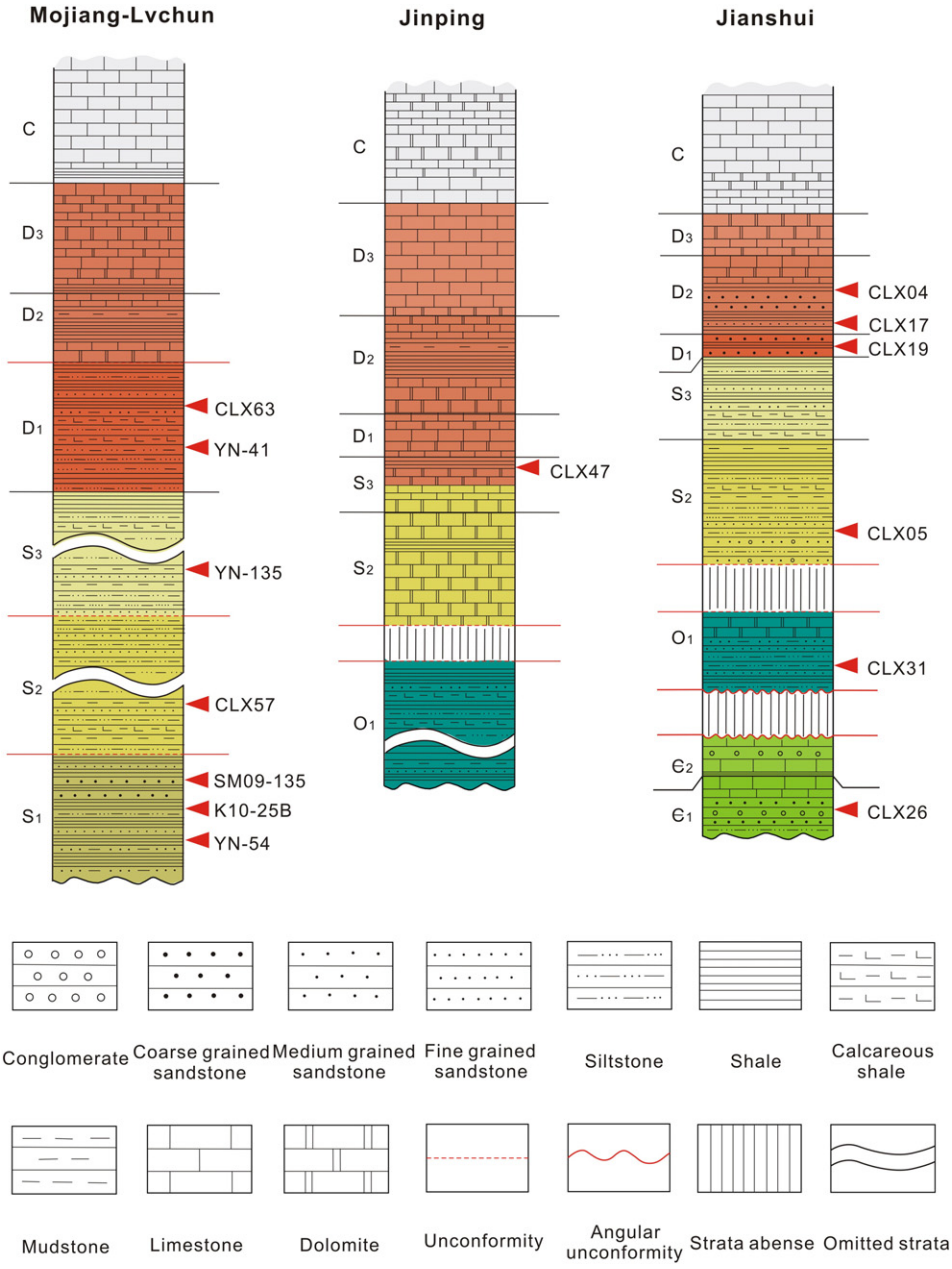

Fig. 3. Simplified Cambrian–Carboniferous stratigraphy at the Jianshui area in the western Yangtze margin, the Mojiang–Lvchun area and Jinping area in the Ailaoshan Belt (modified from YNGMR, 1990). Relative stratigraphic positions of the samples used in this study are indicated.

In the Mojiang–Lvchun area, there is no Cambrian–Ordovician sediments founded. The Silurian–Devonian sediments in this area are mainly composed of pelagic siliciclastic rocks. The Lower Silurian metasediments are largely composed of thick-bedded sandstone interbedded with finely laminated siltstone. The Middle Silurian metasediments are dominated by black shale with pelagic graptolites (Xiong et al., 1998). The Upper Silurian–Devonian strata consist of sandstone, mixed carbonate, minor chert and (recrystallized) mudstone clasts (Pan et al., 2003).

In the Jinping area, Middle Ordovician to Lower Silurian strata are missed. Middle Silurian to Devonian carbonates (with benthonic fossils and some siltstone and shale interbeds) lies unconformity on the Lower Ordovician (calcareous) shale.

The stratigraphy of the western Yangtze margin is well-exposed in the Jianshui area (Fig. 3). The Lower–Middle Cambrian and Lower Ordovician strata comprise mainly carbonates with shale and sandstone interbeds. The Middle Silurian to Devonian sediments comprise neritic sandstone and siltstone with thin limestone interbeds. Upper Cambrian and Middle Ordovician to Lower Silurian strata are absent.

Six Cambrian–Devonian sandstones from western Yangtze and eight Silurian–Devonian sandstones–siltstones from the Ailaoshan Belt (seven from the Mojiang–Lvchun area and one from the Jinping area) were collected for this study. Sample locations and their stratigraphic positions are illustrated in Figs. 2 and 3. Petrographic thin section microphotographs are provided in Fig. 4 and sample description are summarized in Table 1.

3. Analytical methods

Zircons were separated from ca. 5 kg of crushed sample using conventional heavy liquid and magnetic techniques, and hand-picked under a binocular microscope. Out of the 500 zircon grains recovered for each sample, about 200 grains were randomly selected and mounted in epoxy resin,and polished to effectively cut them in half. All zircons

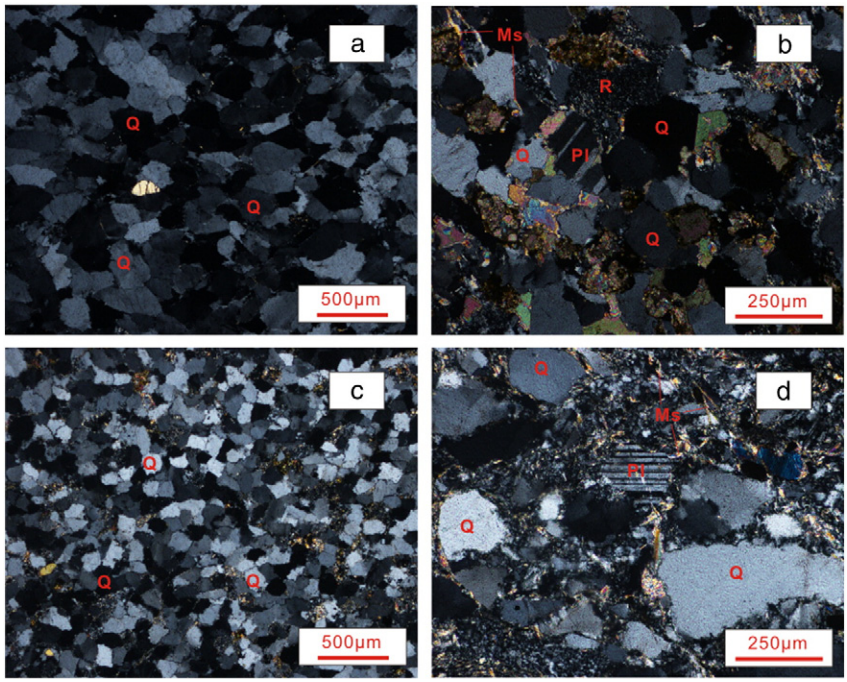

Fig. 4. Thin section petrography of the samples. All images are under cross-polarized light. (a): Sample CLX26; (b): sample CLX05; (c): sample CLX04; (d): sample CLX57. Abbreviations for minerals: Q, quartz; Pl, plagioclase; Ms, muscovite; R, rock fragments.

Table 1
Summarized sample description.

Sample no.	Lithology	Strata age	Mineral composition	Brief description	Source character
Western Yangtze region					
CLX26	Quartz sandstone	Cambrian	Quartz (ca. 95%), feldspar (ca. 3%) and minor heavy minerals	Light grey, medium-grained, subrounded, well sorted	Highly matured, distal, relatively stable
CLX31	Quartz sandstone	Ordovician	Quartz (ca. 93%), minor feldspar (ca. 3%) and minor heavy minerals	Light grey, fine-grained, subrounded, moderately to well sorted	Matured, distal, relatively stable
CLX05	Arkose	Middle Silurian	Quartz (55–65%), feldspar (15–25%), mica (0–10%), lithic fragments (0–5%) and minor heavy minerals	Pink, fine-grained, subangular to subrounded, moderately to poorly sorted	Unmatured, proximal, relatively unstable
CLX47	Calcareous siltstone	Upper Silurian	Quartz (ca. 60%), feldspar (ca. 5%) and lithic fragments (ca. 25%).	Grey, subangular, moderately to poorly sorted	Unmatured, proximal, relatively unstable
CLX19	Arkose	Lower Devonian	Quartz (55–65%), feldspar (15–25%), mica (0–10%), lithic fragments (0–5%) and minor heavy minerals	Pink, fine-grained, subangular, moderately to poorly sorted	Unmatured, proximal, relatively unstable
CLX17	Arkose	Middle Devonian	Quartz (55–65%), feldspar (15–25%), mica (0–10%), lithic fragments (0–5%) and minor heavy minerals	Pink, fine-grained, subangular, moderately to poorly sorted	Unmatured, proximal, relatively unstable
CLX04	Quartz sandstone	Middle Devonian	Quartz (ca. 97%) and minor heavy minerals	Light grey, fine-grained, subrounded, well to moderately sorted	Highly matured, distal, relatively stable
Ailaoshan belt					
SM09-135	Quartz sandstone	Lower Silurian	Grains of quartz (ca. 95%) and minor heavy minerals	Light grey, middle-grained subrounded, well sorted	Highly matured, distal, relatively stable
YN-54	Sublithic arenites	Lower Silurian	Quartz (70–80%), chert and (minor) volcanic lithic clasts (8–15%), feldspar (0–5%) and matrix (5–10%)	Pink, medium-grained, subrounded, moderately to poorly sorted,	Unmatured, proximal, relatively unstable
K10-25B	Sublithic arenites	Lower Silurian	Quartz (65–75%), sedimentary and volcanic lithic clasts (15–20%) and matrix (5–10%)	Pink, fine- to medium-grained subrounded, moderately to poorly sorted,	Unmatured, proximal, relatively unstable
CLX57	Arkoses	Middle Silurian	Quartz (55–65%), feldspar (15–25%), mica (0–10%), lithic fragments (0–5%) and minor heavy mineral	Pink, medium-grained, subangular to subrounded, moderately to poorly sorted	Unmatured, proximal, relatively unstable
YN-135	Sublithic arenites	Upper Silurian	Quartz (60–75%), sedimentary lithic clasts (10–20%) and matrix (0–10%).	Pink, fine- to medium-grained, subrounded, moderately to poorly sorted	Unmatured, proximal, relatively unstable
YN-41	Mylonitic siltstone	Lower Devonian	Quartz (50–60%), feldspar (10–20%), lithic fragments (5–10%), mica (0–5%) and matrix (10–20%)	Pink, fine- to medium-grained, subangular, moderately to poorly sorted	Unmatured, proximal, relatively unstable
CLX63	Quartz sandstone	Lower Devonian	Quartz (ca. 98%) and minor heavy mineral	Light grey, fine-grained, subrounded, well to moderately sorted	Highly matured, distal, relatively stable

were studied under transmitted and reflected light to avoid cracks and inclusions. Cathodoluminescence (CL) images were obtained to characterize the zircon grains in terms of external morphology and internal structure in order to selecting the optimum target sites for U–Pb dating and Hf-isotope analyses.

3.1. Zircon U–Pb dating

U–Pb measurements of samples K10-25B, SM09-135, YN-41, YN-54 and YN-135 were analyzed by use of an Agilent 7500cs quadrupole ICPMS coupled with a RESOlution M-50 193 nm Excimer laser ablation (LA) system at the Centre of Excellence in Ore Deposits (CODES) in the University of Tasmania. The down-hole fractionation, instrument drift and mass bias correction factors for Pb/U ratios on zircons were determined by 91500 zircon standard (Wiedenbeck et al., 1995) and checked using the standard zircon Temora (Black et al., 2003), GJ1 (Jackson et al., 2004) and the Mud Tank Zircon (Black and Gulson, 1978). The correction factors for the $^{207}Pb/^{206}Pb$ ratio was calculated using analyses of NIST610 analyzed throughout the day and calculated using the recommended values by (Baker et al., 2004). Each analysis began with a 30 s blank gas measurement followed by a further 30 s analysis time when the laser was switched on. The zircon was sampled on a 32 μm spots using a laser repetition at 5 Hz and a density of approximately 2 J/cm^2. A flow of He carrier gas at a rate of 0.6 l/min was used to carry particles ablated by the laser out of the chamber to be mixed with Ar gas and flowed to the plasma torch finally. Isotopes measured for zircons were ^{90}Zr, ^{181}Hf, ^{202}Hg, ^{204}Pb, ^{206}Pb, ^{207}Pb, ^{208}Pb, ^{232}Th, and ^{238}U.

U–Pb analysis of the other samples were conducted using a Neptune plus multi-collector inductively coupled plasma mass spectrometer (MC–ICP–MS) with RESOlution M-50 193 nm laser ablation system at the State Key Laboratory of Isotope Geochemistry, Guangzhou Institute of Geochemistry, Chinese Academy of Sciences (GIGCAS). The equipment configuration details were provided by Xia et al. (2013).

Zircons were sampled on 24 or 33 μm spots using the focused UV laser at 4 Hz and a density of approximately 80 mJ/cm^2, and the ablated material was carried by a continuous flow of He at a rate 0.5 l/min out of the chamber to be mixed with Ar gas and transferred to the ICP-MS for quantification. Every spot analysis consisted of approximately of 30 s gas blank measurement and 30 s sample data acquisition. Raw count rates were measured for ^{202}Hg, ^{204}Pb, ^{206}Pb, ^{207}Pb, ^{208}Pb, ^{232}Th, ^{235}U, ^{238}U. No common lead correction has been made because the common lead composition cannot be measured accurately due to its very low counts (204Pb) and interference from 204Hg in gas. Harvard zircon 91500 (Wiedenbeck et al., 1995) was used to calibrate the U–Th–Pb ratios and absolute U abundances. The zircon standards Plesovice (Sláma et al., 2008) and Temora (Black et al., 2003) were used as monitoring unknown samples. They always gave ages within 3% error of their recommended values. All the age calculations and plotting of diagrams were made using ISOPLOT 3.0 (Ludwig, 2003).

3.2. Lu–Hf isotope analyses

In situ Hf isotopic analysis was conducted using a LA–MC–ICP–MS at the State Key Laboratory of Isotope Geochemistry, GIGCAS, same with that for U–Pb dating. Lu–Hf isotopic measurements were performed subsequently on the same spots or the same age domains of zircon grains with concordant U–Pb age (discordance <5%). Measuring settings mainly include ablation spots of 44 μm, repetition rate of 4–5 Hz, and laser beam energy density of 80 mJ/cm^2 and ablation time of 30s. Masses acquired for Hf isotope are 180–175, 171 and 173. Measured isotope ratio of $^{176}Hf/^{177}Hf$ were normalized to $^{179}Hf/^{177}Hf = 0.7325$, using exponential correction for mass bias. Isobaric interference of ^{176}Yb and ^{176}Lu on ^{176}Hf was corrected by monitoring ^{173}Yb and ^{175}Lu, respectively. In situ measured $^{173}Yb/^{171}Yb$ ratio is used for mass bias correction for both Yb and Lu because of their similar physicochemical properties. Ratios used for the corrections are 0.7963 of $^{176}Yb/^{173}Yb$ and 0.02655 of $^{176}Lu/^{175}Lu$ (Vervoort et al., 2004). The zircon standard Penglai (Li et al., 2010) were also analyzed twice about every hour as unknown to check the reliability of the method and its results were found always within ±1.5 εHf units error of the recommended values.

The decay constant for ^{176}Lu of 1.867×10^{-11}/year (Scherer et al., 2001) was used to calculate initial $^{176}Hf/^{177}Hf$ ratios. The present-day chondritic values of $^{176}Hf/^{177}Hf = 0.282785$ and $^{176}Lu/^{177}Hf = 0.0336$ (Bouvier et al., 2008), and zircon ages determined by U–Pb dating techniques were used for calculating $\varepsilon Hf(t)$. Two types of Hf model ages, T_{DM1} and T^C_{DM}, were calculated from the measured U–Pb ages and Lu–Hf isotopes of the zircons. Single-stage model ages (T_{DM1}) which represent a minimum age for the source material of the zircon parental magma were calculated relative to depleted mantle with a present-day $(^{176}Lu/^{177}Hf)_{DM} = 0.0384$ and $(^{176}Hf/^{177}Hf)_{DM} = 0.28325$ (Griffin et al., 2000). Two-stage model ages (T^C_{DM}) were calculated assuming that zircon parental magma was produced from an average continental crust, with $^{176}Lu/^{177}Hf = 0.015$, that originated from the depleted mantle source (Griffin et al., 2002). We believe that it provides a more realistic estimate of its source age.

4. Results

Total 9 samples (CLX04, CLX05, CLX17, CLX19, CLX26, CLX31, CLX47, CLX57 and CLX63) were analyzed in this study. Although the results of another five samples (K10-25B, SM09-135, YN-41, YN-54 and YN-135) analyzed by Lai (2012) had been contributed to the SE Asian detrital zircon statistical studies of Burrett et al. (2014), detail analytical data, petrographic descriptions, detrital zircon age patterns and provenance of these Ailaoshan samples are first mentioned and discussed in this paper. All U–Pb ages and Lu–Hf isotope data obtained in this study are listed in the electronic supplement as Tables S1 and S2. CL images of representative zircons are shown in Fig. 5. Uncertainties of individual analyses reported in the data table and concordia plots are presented at 1σ level. In this paper, all analyses are shown by the concordia plots of Fig. 6, but the analyses with discordance greater than 5% are rejected for further consideration. The $^{207}Pb/^{206}Pb$ age is used for zircons older than 1000 Ma and $^{206}Pb/^{238}U$ age for those younger than that.

Most of the analyzed zircons are colorless and transparent while some have colors of light pink to brown. The zircon grains are 40 um to 250 um long with aspect ratios of 1:1 to 3:1. Most of them have clear oscillatory CL zoning (Fig. 5) and high Th/U ratio (Table S1), indicating their magmatic origin (Corfu et al., 2003).

4.1. Western Yangtze margin

4.1.1. Sample CLX26

76 detrital zircon grains from this sample have been analyzed and yielded 67 concordant (discordance <5%) ages. These concordant ages have a range from Neoproterozoic to latest Neoarchean (ca. 616–2510 Ma) with two major peaks at ca. 872 Ma and 1565 Ma, two minor peaks at ca. 1180 Ma, ca. 2490 Ma, and one broad age group between 1720 and 1820 Ma (Figs. 6a and 7a).

Hf isotope analyses of 44 zircons were made for this sample. The grains within the 872 Ma age peak (752–904 Ma) have $\varepsilon Hf(t)$ values ranging from −10.11 to +11.07 and T^C_{DM} model ages from 1.05 to 2.66 Ga. Zircons with ages of 1556–1681 Ga have $\varepsilon Hf(t)$ values of −7.62 to +5.16 and corresponding T^C_{DM} model ages from 1.97 to 2.87 Ga, and the 2263–2510 Ma zircons have $\varepsilon Hf(t)$ values of −8.28 to +1.65 with T^C_{DM} model ages from 2.93 to 3.54 Ga.

4.1.2. Sample CLX31

80 detrital zircon grains from this sample have been analyzed and 56 concordant ages were yielded varying from 535 ± 13 to 3087 ± 20 Ma (Fig. 6b). The ages mainly cluster in the range of 730 to 900 Ma with a

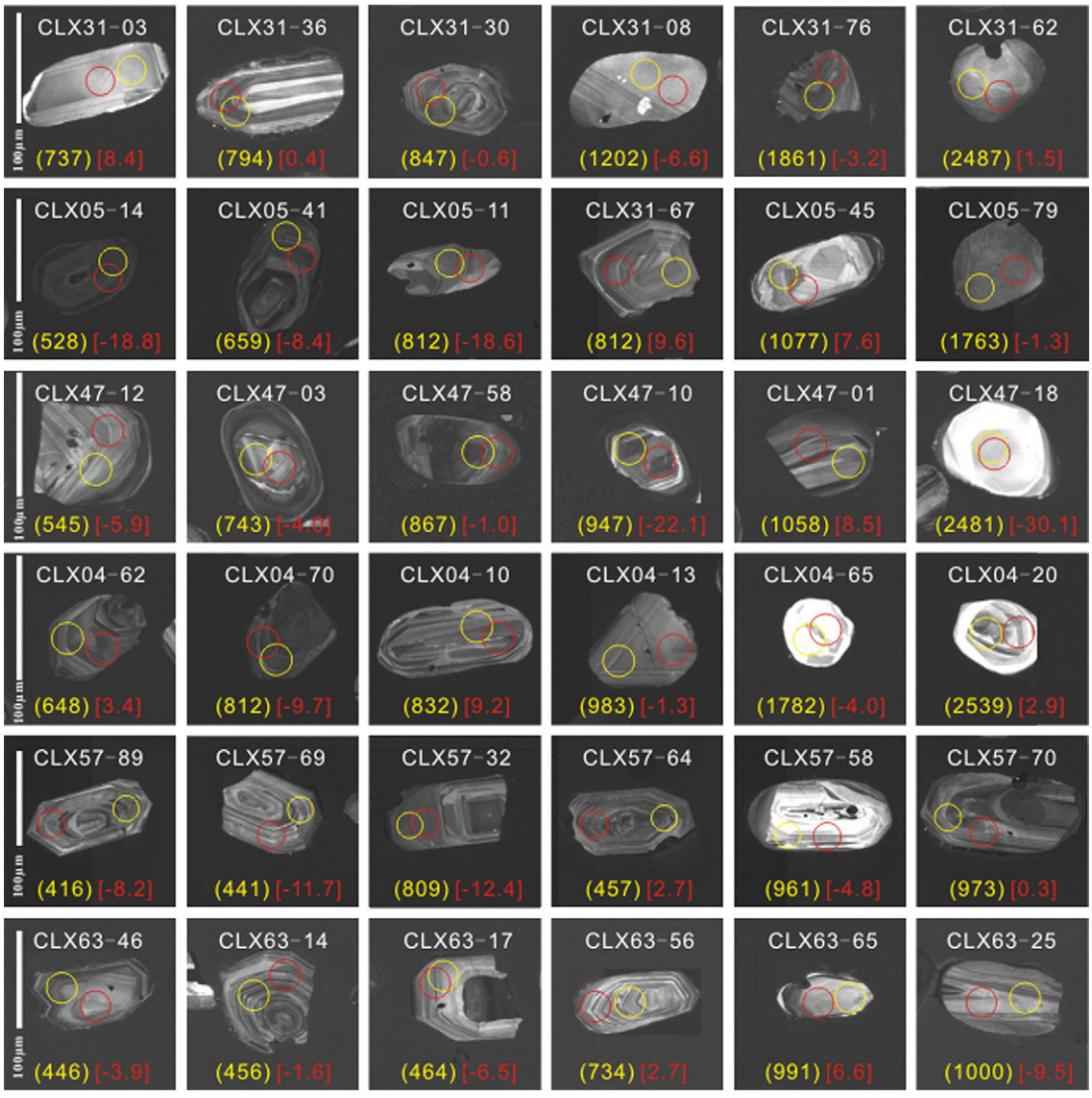

Fig. 5. CL images of selected detrital zircons analyzed in this study. Analytical spots and data for U–Pb (yellow) and Lu–Hf (red) isotopes are shown.

major peak at 810 Ma and a number of subordinate peaks at ca 540 Ma, ca 1560 Ma, ca 1690 Ma and ca 2490 Ma are shown (Figs. 6b and 7b).

Fifty-one dated zircons from this sample were analyzed for Hf isotopes. The zircon population within the 810 Ma age peak (730–904 Ma) exhibit negative to positive $\varepsilon Hf(t)$ values of −8.64 to +9.89, yielding T_{DM}^{C} model ages ranging from 1.13 to 2.22 Ga. The $\varepsilon Hf(t)$ and T_{DM}^{C} values for the age population of 1451–1717 Ma range from −13.79 to +4.21 and from 2.02 to 3.27 Ga, respectively. For the 2455–2542 Ma zircon population, the $\varepsilon Hf(t)$ values are +0.56 to +4.07 and the T_{DM}^{C} values are 2.80–2.96 Ga.

4.1.3. Sample CLX05

76 detrital zircon grains analyzed for this sample has yielded 54 concordant ages (ca. 502–1763 Ma) and three age populations with age peaks at ca. 540 Ma, ca. 640 Ma and ca. 810 Ma can be recognized (Figs. 6c and 7c).

Forty-two zircons with concordant ages were analyzed for Hf isotopes. The 502–669 Ma zircons all have negative $\varepsilon Hf(t)$ values from −20.79 to −2.68 and T_{DM}^{C} model ages from 1.73 to 2.81 Ga, although one analysis has a positive $\varepsilon Hf(t)$ value of +1.66 and T_{DM}^{C} model age of 1.45 Ga, indicating that their parent magmas were produced by reworking of 1.45–2.8 Ga continental crust. The 785–889 Ma zircons have highly variable $\varepsilon Hf(t)$ values from −29.18 to +13.55, and corresponding large range of T_{DM}^{C} model ages from 0.91 to 3.53 Ga.

4.1.4. Sample CLX19

80 detrital zircon grains ($n = 80$) analyzed for this sample have yielded 63 concordant ages (ca. 605–2334 Ma) with a dominate age peak at ca. 830 and a shoulder age peak at ca. 970 Ma (Figs. 6e and 7e).

Hf isotope analyses of 63 age concordant zircons were made for this sample. The grains within the 830 Ma age peak (706–905 Ma) have $\varepsilon Hf(t)$ values from −16.90 to +11.15 and model ages of 1.08–2.79 Ma (most are 1.1–1.7 Ga). Fifteen detrital zircons with ages of ca 970 Ma have $\varepsilon Hf(t)$ values from −13.39 to +12.10 and a large range of T_{DM}^{C} model ages from 1.04 to 2.69 Ga.

4.1.5. Sample CLX17

A total of 69 detrital zircon U–Pb analyses were conducted for this sample, which yielding 50 concordant ages ranging from 553 ± 13 to 2698 ± 20 Ma. The ages mainly cluster in the range of 550 to 1050 Ma and two major peaks at ca. 835 Ma and ca. 935 Ma are recognized. There are also one subordinate peak at ca. ca. 1610 Ma and one broad age group between 2420 and 2510 Ma (Figs. 6f and 7f).

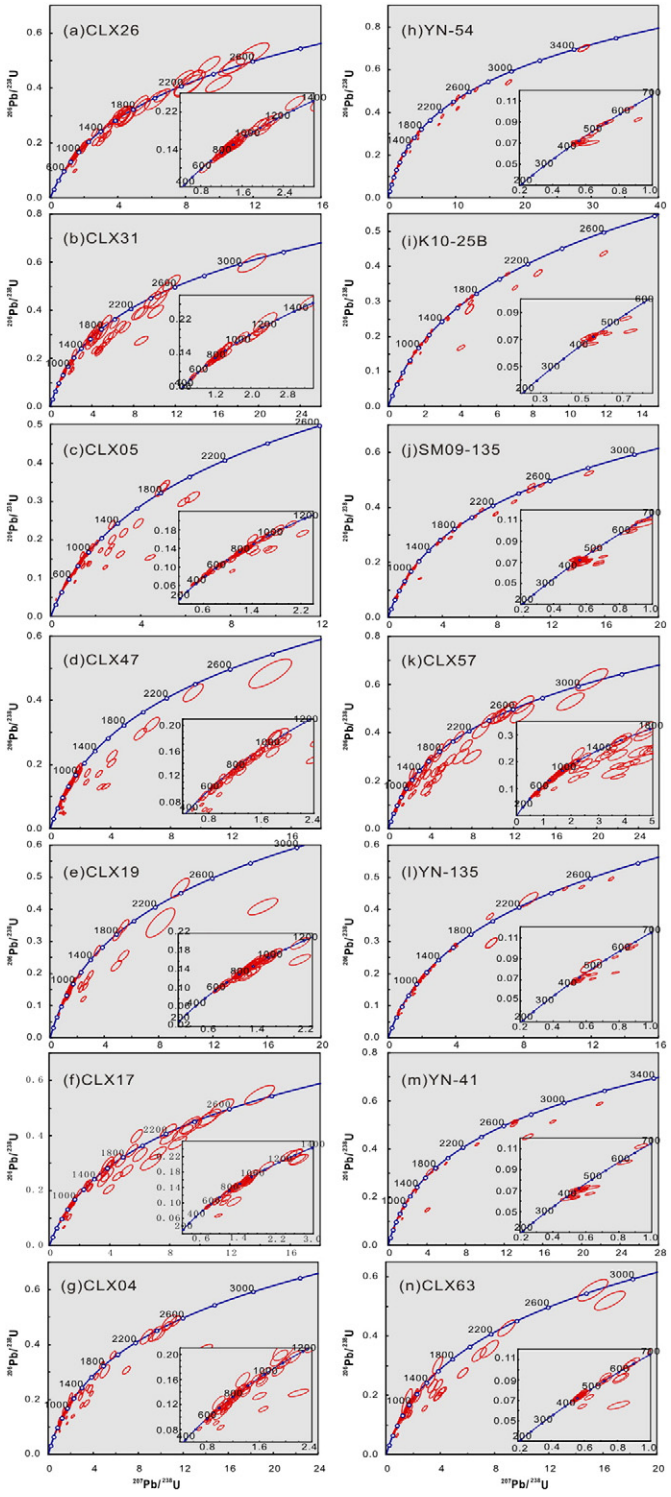

Fig. 6. U–Pb concordia diagrams of detrital zircon analytical results. Errors are quoted in 1σ level.

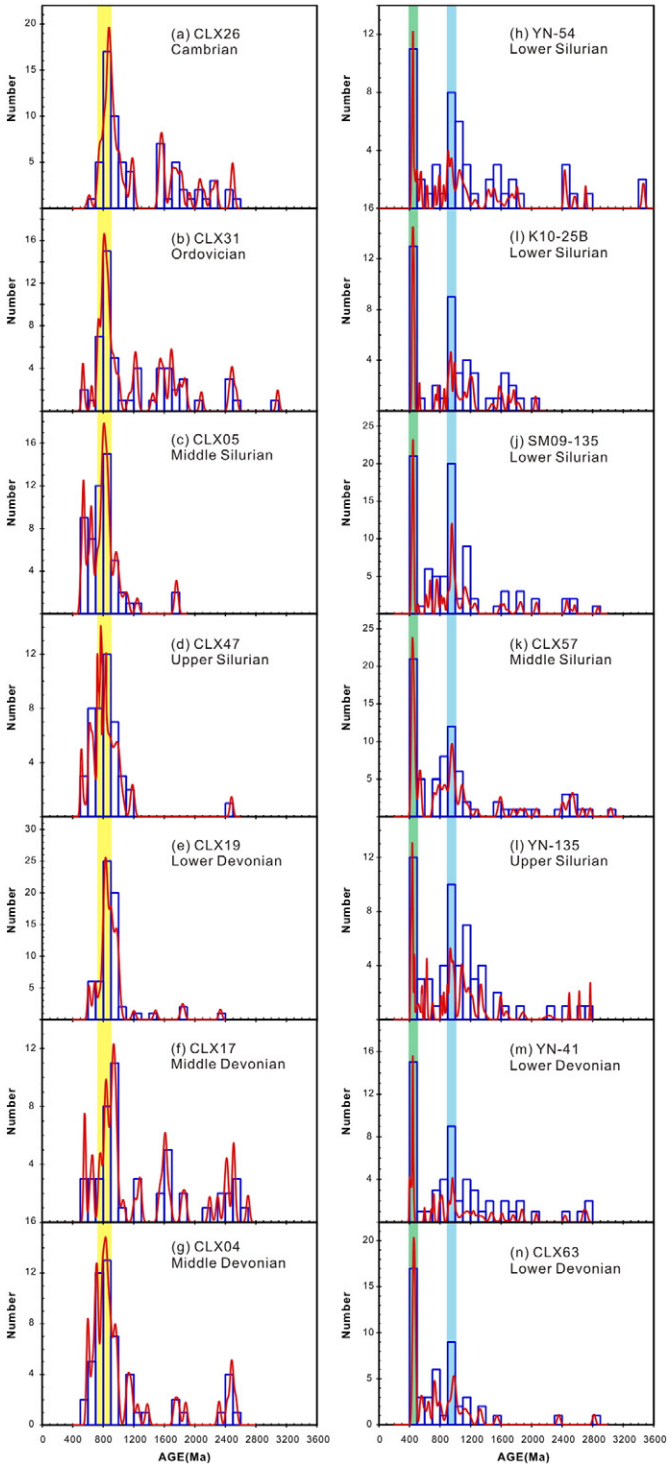

Fig. 7. Detrital zircon U–Pb age histograms. Only ages with lower than 5% discordance are used. The light green and light blue bars show the diagnostic age peaks for an Indochina–Simao provenance, whereas the yellow bar shows that for a Yangtze provenance.

Hf isotopic analyses on 46 zircons were undertaken for this sample. Zircons with ages of 745–900 Ma have both negative and positive $\varepsilon Hf(t)$ values (−11.82 to +10.48), which correspond to T^C_{DM} model ages from 1.07 to 2.48 Ga. The 904–996 Ma zircons have $\varepsilon Hf(t)$ values from −2.19 to +11.0, mostly positive. Their T^C_{DM} model ages are 1.13–1.93 Ga. Eight grains with ages of ca 1610 Ma have $\varepsilon Hf(t)$ values from −7.37 to +9.97 and T^C_{DM} model ages from 1.78 to 2.93 Ga. The zircons with U–Pb age of 2223–2748 Ma yield a T^C_{DM} model age of 2.90–3.71 Ga.

4.1.6. Sample CLX04

79 detrital zircon grains from this sample has yielded 54 concordant ages (ca. 590–2539 Ma) with a significant age peak at ca. 830 Ma. Minor age peaks are shown at ca. 720 Ma, ca. 960 Ma and ca. 2480 Ma (Figs. 6g and 7g).

Hf isotopic analyses of 48 zircons were undertaken for this sample. The 705–900 Ma zircons have $\varepsilon Hf(t)$ values from −19.47 to +15.88 with T^C_{DM} model ages of 0.72–2.96 Ga. Zircons with ages

of 916–1378 Ma have $\varepsilon Hf(t)$ values between −24.92 and +11.51, which correspond to model ages from 1.02 to 3.38 Ga. The Paleoproterozoic zircons have $\varepsilon Hf(t)$ values of −14.32 to +8.18 and T_{DM}^{C} model ages from 1.92 to 3.87 Ga.

4.2. Ailaoshan Belt

4.2.1. Sample YN-54

A total of 61 analytical zircon U–Pb results were obtained for this sample, of which 49 results are concordant with ages from 427 ± 7 to 3465 ± 17 Ma. A large cluster of ages distribute between 400 and 500 Ma with a prominent peak at ca. 445 Ma. Subordinate ages are spanned from ca. 900 to ca. 964 Ma.

4.2.2. Sample K10-25B

A total of 54 detrital zircon U–Pb analyses were undertaken on this sample, which produced 44 concordant ages varying from 430 ± 6 to 2053 ± 14 Ma. Among the 44 concordant analyses, 13 zircons are dated at 400–500 Ma, forming a pronounced age peak at ca. 440 Ma. Another significant age peak is shown at 945 Ma. A number of subordinate age peaks are present at ca. 1200 Ma, ca. 1575 Ma, ca. 1765 Ma and one broad age group between 900 and 1050 Ma (Figs. 6i and 7i).

4.2.3. Sample SM09-135

A total of 98 detrital zircon U–Pb analyses were conducted for this sample, which yielded 83 concordant results with ages from 423 ± 5 to 2870 ± 15 Ma. There are two significant age peaks at ca. 445 Ma and ca. 960 Ma, along with three subordinate age peaks at ca. 670 Ma, ca. 740 Ma and ca. 1130 Ma (Fig. 6j and 7j).

4.2.4. Sample CLX57

119 detrital zircons were analyzed for this sample, which yielded 77 concordant ages (ca. 418–2668 Ma) with two major peaks at ca. 440 Ma and 960 Ma (Figs. 6k and 7k).

Sixty dated concordant zircons from this sample were analyzed for Hf isotopes. The major zircon population at 415–490 Ma zircons have $\varepsilon Hf(t)$ values from −10.83 to +13.63 with a large range of T_{DM}^{C} model ages from 0.58 to 2.17 Ga, suggesting that the zircons crystallized from different magmas at a similar time. Zircons with ages of 919–988 Ma have $\varepsilon Hf(t)$ values between −9.35 and +0.29, which correspond to T_{DM}^{C} model ages from 1.79 to 2.42 Ga.

4.2.5. Sample YN-135

A total of 64 detrital zircon U–Pb analyses were undertaken on this sample, which yielded 57 concordant ages ranging from 413 ± 4 to 2769 ± 5 Ma. There are two major age peaks at ca. 435 Ma and ca. 950 Ma, along with two subordinate age peaks at ca. 1090 Ma and ca. 1330 Ma (Figs. 6l and 7l).

4.2.6. Sample YN-41

A total of 70 detrital zircon U–Pb analyses were conducted for this sample. 54 concordant ages were obtained, which vary from 400 ± 5 to 2678 ± 15 Ma. This sample contains two major populations of zircon ages with peaks at ca. 445 and ca. 965 (Figs. 6m and 7m).

4.2.7. Sample CLX63

78 detrital zircon grains from this sample were analyzed for their U–Pb ratios, which yield 49 concordant ages (ca. 435–2819 Ma) with two major peaks at ca. 455 Ma and ca. 974 Ma (Figs. 6n and 7n).

A total of 47 zircons were analyzed for their Hf isotope composition. The 435–484 Ma zircons have $\varepsilon Hf(t)$ values from −15.24 to 0.40 with a narrow range of T_{DM}^{C} model ages from 1.42 to 2.41 Ga, indicating that their parent magmas were mainly produced by reworking of continental crust. The other major zircon population with ages of 901–985 Ma have $\varepsilon Hf(t)$ values from −11.34 to +6.63 and T_{DM}^{C} model ages from 1.41 to 2.54 Ga.

4.2.8. Sample CLX47

A total of 68 detrital zircon U–Pb analyses were obtained for this sample, which produced 47 concordant ages ranging from 508 ± 12 to 2481 ± 20 Ma. The ages can be grouped into two distinct population: 540 Ma to 700 Ma and 730 Ma to 900 Ma. Other subordinate age peaks include ca. ca 956 Ma, and ca. 1180 Ma (Figs. 6d and 7d).

In total, 17 zircons from this sample were analyzed for Hf isotopes. The 508–633 Ma zircons have $\varepsilon Hf(t)$ values from −17.03 to +2.04 and T_{DM}^{C} model ages from 1.45 to 2.56 Ga. The 738–900 Ma zircons have $\varepsilon Hf(t)$ values from −5.44 to +10.08, and a corresponding large range of T_{DM}^{C} model ages from 1.14 to 2.02 Ga. The 916–1086 Ma zircons have $\varepsilon Hf(t)$ values from −23.78 to +8.49 and T_{DM}^{C} model ages from 1.33 to 3.31 Ga.

5. Discussion

5.1. Detrital provenance

5.1.1. Western Yangtze margin

The most important feature of detrital zircon U–Pb age pattern for the six Cambrian to Devonian siliciclastic samples from the western Yangtze margin (i.e., CLX04, CLX05, CLX17, CLX19, CLX26 and CLX31) is that they share a pronounced detrital zircon age peaks of ca. 730–900 Ma (as indicated by the yellow bar in Fig. 7). These detrital zircons of 730–900 Ma are characterized by both negative and positive $\varepsilon Hf(t)$ values (Figs. 8 and 9). In western Yangtze, there are a lot of Neoproterozoic mafic intrusions (Fig. 1) (Z. Li, 2003; Zhu et al., 2006; Zhao and Zhou, 2007; Zhu et al., 2008; Cai et al., 2014) and intermediate-acid intrusions (Fig. 1) (Li et al., 2002; Zhou et al., 2002a; X. Li, 2003; Z. Li, 2003; Zhou et al., 2006; Huang et al., 2008; Liu et al., 2008; Zhao et al., 2008; Wang et al., 2011; Lin et al., 2012) in the Pangzhihua–Yuanyang region. In addition, many Neoproterozoic felsic to mafic plutons have also been reported in the Hannan region along the northern margin of the Yangtze Block (Fig. 1) (Zhou et al., 2002b; Yan et al., 2004; Wang et al., 2008; Zhao and Zhou, 2008; Pei et al., 2009; Zhao and Zhou, 2009; Zhao et al., 2010; Dong et al., 2011, 2012; Zhao et al., 2013). However, there is no Neoproterozoic magmatism has been reported within the Indochina–Simao Block. Therefore, the widespread Neoproterozoic igneous rocks along the western Yangtze margin could be the source of those detrital zircons within the age peak of 730–900 Ma. This also is consistent with previous studies on the Neoproterozoic to Devonian sedimentary rocks from the Yangtze Block, which have indicated that their provenances are characterized by a pronounced age group at 730–900 Ma (Fig. 10a)

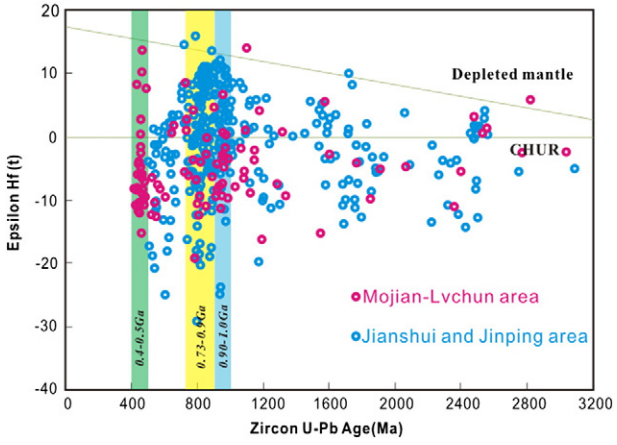

Fig. 8. A plot of $\varepsilon Hf(t)$ vs. U–Pb ages for the detrital zircons from this study. Hf-isotope evolution line for Depleted Mantle follows Griffin et al. (2000).

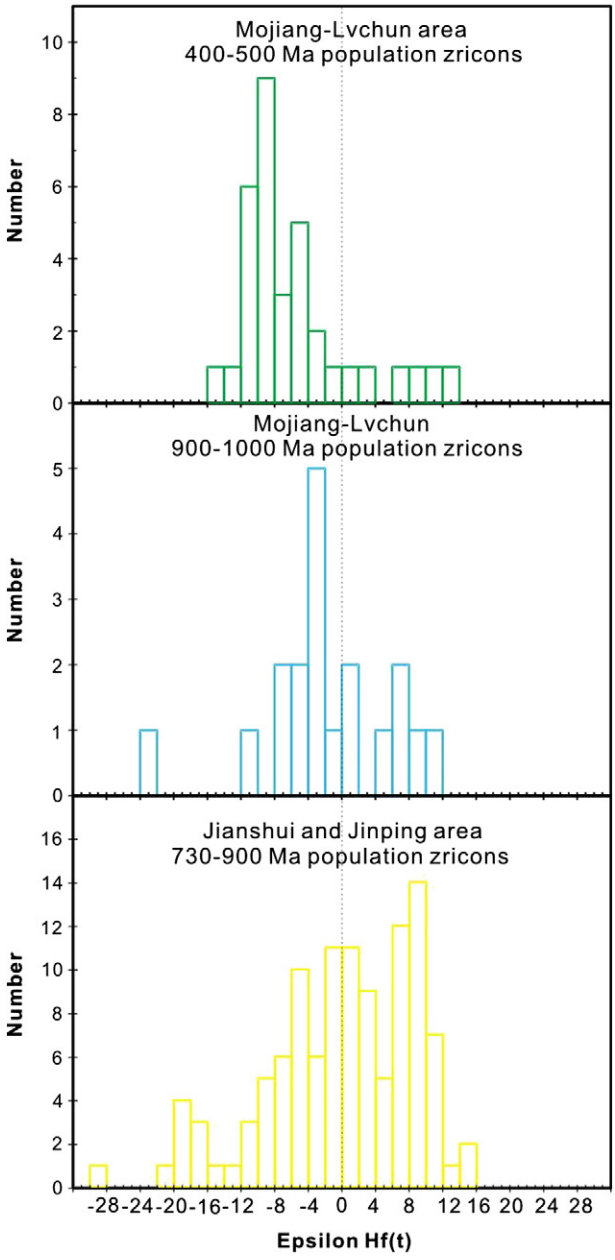

Fig. 9. Plots of $\varepsilon Hf(t)$ histograms for the diagnostic age peaks from the Ailaoshan Belt and the Yangtze Block.

(Greentree et al., 2006; Sun et al., 2009; Duan et al., 2011; Wang et al., 2012; Q.F. Wang et al., 2014). It is worthy to note that although previous studies on intrusions (e.g., Cai et al., 2014) indicate that most Neoproterozoic zircons in western margin of the Yangtze Block have positive $\varepsilon Hf(t)$ values, both positive and negative $\varepsilon Hf(t)$ values are shown for the detrital zircons with Neoproterozoic ages in our study. Previous detrital zircon data have also shown that Neoproterozoic zircons have both positive and negative $\varepsilon Hf(t)$ values (e.g. Dong et al., 2011; Duan et al., 2011; Wang et al., 2012; Xu et al., 2013; Q.F. Wang et al., 2014; Zhou et al., 2015). These data may imply that Neoproterozoic intrusions with negative zircon $\varepsilon Hf(t)$ values in the Yangtze Block may have more exposure before than that today.

Other zircon U–Pb age peaks such as 530–650 Ma and 2400–2500 Ma are only appear in part of the samples from the western Yangtze margin (Fig. 7). Detrital zircon population of 530–650 Ma appears mainly in the Middle Silurian to Middle Devonian sequence and associated generally with negative $\varepsilon Hf(t)$ values (Fig. 8), implying reworking of older crustal material. Although no igneous rocks with 530–650 Ma have yet been identified in South China, abundant detrital zircons of this age have been widely reported in Upper Neoproterozoic to Cambrian sequence in both the Yangtze and Cathaysia blocks (Wang et al., 2012; Xu et al., 2013; Zhou et al., 2015). These sedimentary rocks can supply the detrital zircons with age 530–650 Ma. However, these detrital zircons may also derive directly from the Pan-African orogenic belt associated with the formation of the Gondwana supercontinent. Previous studies on lower Paleozoic detrital sedimenatry rocks in the South China Block have also found abundant detrital zircons with Pan-African age and concluded that the South China Block should be linked with and received detritus from North India and Western Australia during the assembly of East Gondwana. Our new data is consistent with and provided more evidence for this conclusion (Wang et al., 2012; Xu et al., 2013; Zhou et al., 2015).

The oldest detrital zircon population (2400–2500 Ma) have a wide range of $\varepsilon Hf(t)$ values from −15 to +5 with T_{DM}^{C} model ages varying from 2.8 to 3.2 Ga (Fig. 8). Although magmatic and metamorphic events in the period are not well known in the Yangtze Block, detrital zircons of these ages have also been widely reported in Precambrian metasedimentary rocks, which may have been potential detrital sources for our western Yangtze samples (Greentree et al., 2006; Greentree and Li, 2008; Sun et al., 2009; Wang et al., 2012).

As a comparison, we have compiled previously published detrital zircon age data for the Neoproterozoic to Devonian sedimentary rocks derived from the Yangtze block, it shows a pronounced age peak at ca. 812 Ma (Fig. 10b), very similar with that for our samples. As for the Hf model age (T_{DM}^{C}), our results for those detrital zircons from the west margin of the Yangtze block have a T_{DM}^{C} age peak at ~1.8 Ga. This is also similar to that for the detrital zircons from the Cambrian and Devonian sedimentary rocks in the inland South China (Fig. 11). Therefore, we suggest that the Yangtze Block was the main detrital source for Cambrian–Devonian siliciclastic rocks along the western Yangtze margin.

5.1.2. Ailaoshan Belt

The seven sandstones–siltstones (i.e., CLX57, CLX63, K10-25B, SM09-135, YN-41, YN-54 and YN-135) collected from the Mojiang–Lvchun area are characterized by two prominent U–Pb age peaks at 400–500 and 900–1000 Ma and significant crustal additions at around 2.1Ga (Figs. 6, 7 and 11a). In contrast, the siltstone (i.e., CLX47) collected from the Jinping area displays a totally different age pattern with a peak at 730–1000 Ma (Figs. 6 and 7). Therefore, detrital provenances of these two areas were likely to be very different.

The 400–500 Ma detrital zircons in the Mojiang–Lvchun area are mostly euhedral and have Th/U ratios > 0.1. They have a wide range of $\varepsilon Hf(t)$ values from −15 to +5, yet most data (82.4%) are negative (Figs. 8 and 9). In the Ailaoshan–Jinshajiang Belt, the Gongbo gabbro/diabase have been dated to be Late Ordovician to Silurian (U–Pb zircon: 423–451 Ma) (Jian and Zhong, 2002), whilst the Jinshajiang amphibolite has been dated to be Silurian–Early Devonian (U–Pb zircon: 401–443 Ma) (Jian et al., 2009b). Although there is no Hf isotope data reported for these rocks, rarely crystalline of zircons and limited distribution makes them unlikely to be the source of the widely occurred 400–500 Ma detrital zircons.

The Simao Block is largely covered by Mesozoic and Cenozoic red beds (YNGMR, 1990; L. Wang et al., 2014) and its basement information is rare. However, Ordovician–Silurian mafic–felsic rocks with arc affinity have been found on the western edge of Indochina–Simao Block, from north to south, including the 439–443 Ma (U–Pb zircon) gabbro at Nantinghe (B.D. Wang et al., 2013), 418–421 Ma (U–Pb zircon) basalt–andesite–dacite–rhyolite at Dazhonghe (Mao et al., 2012), 456–459 Ma (U–Pb zircon) basalt–andesite–dacite–rhyolite at Huiming (Nie et al., 2015), 429 ± 3 Ma (U–Pb zircon) dacite–rhyolite at Dapingzhang (Lehmann et al., 2013), 428 ± 7 Ma (U–Pb zircon) rhyolitic tuff at Sang Khom and 434 ± 4 Ma (U–Pb zircon) rhyolitic tuff at Pak

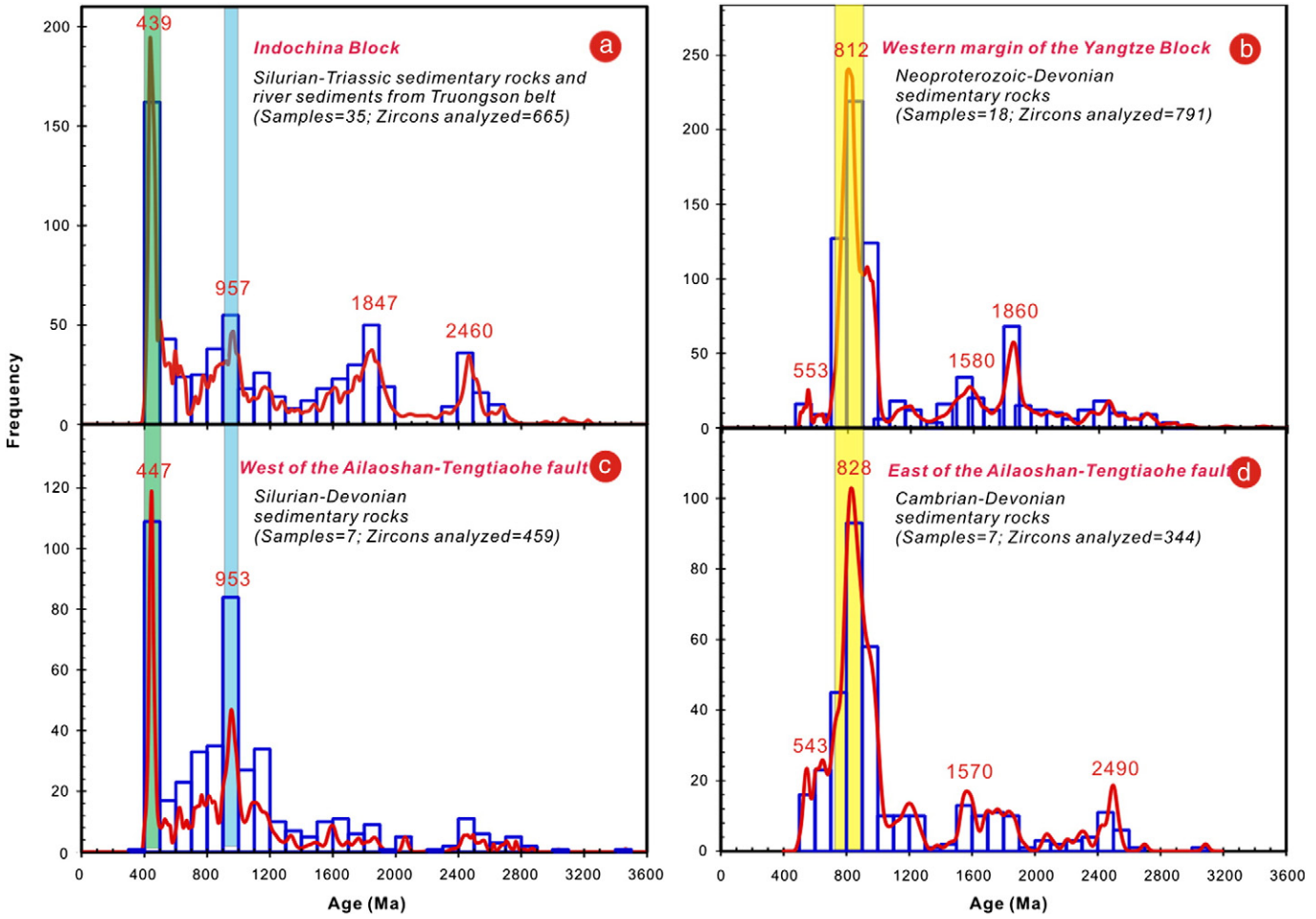

Fig. 10. Summary of detrital zircon age distributions of sedimentary rocks of this study and previous works. (a) Compilation of detrital zircon age data from the western Yangtze margin (Greentree et al., 2006; Sun et al., 2009; Duan et al., 2011; Wang et al., 2012; Q.F. Wang et al., 2014). (b) Compilation of detrital zircon age data from Indochina (Usuki et al., 2013; Burrett et al., 2014). (c) Compilation of the samples in this study from east of the Ailaoshan–Tengtiaohe fault. (d) Compilation of the samples in this study from west of the Ailaoshan–Tengtiaohe fault. Important age peaks are shown in color bands: the light green, yellow and light blue bars represent the 400–500 Ma, 730–900 Ma and 900–1000 Ma age group, respectively.

Chom (Khositanont et al., 2008). Available Hf isotope data for the Huiming dacite-rhyolite (−4.41 to −3.2) (Nie et al., 2015) are consistent with our detrital zircon data (Fig. 8). Besides, ca. 400–470 Ma (U–Pb zircon) granitoids and high-grade metamorphic rocks have also reported in the central Vietnam (Nagy et al., 2001; Tran and Nguyen, 2006; Tran et al., 2014). In addition, most of the 400–500 Ma zircons in this study have subhedral morphology (Fig. 4), implying short-distance transportation from their source regions. Therefore, it is more likely that the source of these 400–500 Ma zircons lies within the Indochina–Simao Block.

The 900–1000 Ma zircons are subrounded or rounded shapes, suggesting strong ablation during long-distance transport. Combining with no counterpart igneous bodies of these ages have been recognized in Indochina–Simao, we infer that these zircons of this study mostly represent exotic input from other adjacent continental terranes. Considering the Indochina–Simao Block located along the northern margin of East Gondwana in Silurian–Devonian (Metcalfe, 2013; Usuki et al., 2013; Burrett et al., 2014), the Rayner–Eastern Ghats belt in India and Antarctic with ca. 900–990 magmatic events can be the potential source of the 900–1000 Ma detrital zircons in our samples.

Previous detrital zircon analyses on Silurian–Triassic siliciclastics and modern river sediments from the Indochina have indicated a pronounced age peak at ca. 439 Ma and at ca. 957 Ma (Fig. 10a, Usuki et al., 2013; Burrett et al., 2014). This character is very similar with our data, although previous data have more significant Archean peaks (Fig. 10b). Based on these data, we suggest that the Silurian–Devonian siliciclastic rocks in the Mojiang–Lvchun area may share the same detrital provenance with the siliciclastics in the Indochina Block which may derived from the Indochina Block and the northern East Gondwana.

In contrast, detrital zircon age pattern of the Upper Silurian siltstone (sample CLX-47) from the Jinping area is similar to those of the Lower Paleozoic western Yangtze siliciclastic rocks, especially for the Middle Silurian sandstone sample CLX-05. Therefore, we suggest that the Lower Paleozoic Jinping area and the Yangtze Block may have shared similar detrital provenance and connected or very close to each other at that time.

5.2. New insights on delineating the Yangtze/Indochina–Simao suture zone

Since the Cenozoic Ailaoshan fault is spatially closely associated with the ophiolite belt in the north (Leloup et al., 1995), this whole fault has been traditionally taken as the suture of the Ailaoshan Ocean (Sone and Metcalfe, 2008). Alternatively, some researchers suggested that the suture may lie along the Lixiangjiang fault (>50 km west of the Ailaoshan fault, Chung et al., 1997; Xiao et al., 2003; Wang et al., 2007). These researchers have demonstrated that the Jinping–Song Da basalts belong to the Late Permian (~260 Ma) ELIP, which occurred prior to the closure of the Ailaoshan Ocean. Therefore, the Jinping area was likely to be connected to South China (rather than to the rest of the Ailaoshan Belt) and thus the Ailaoshan fault cannot be the suture. Recently, detrital zircon

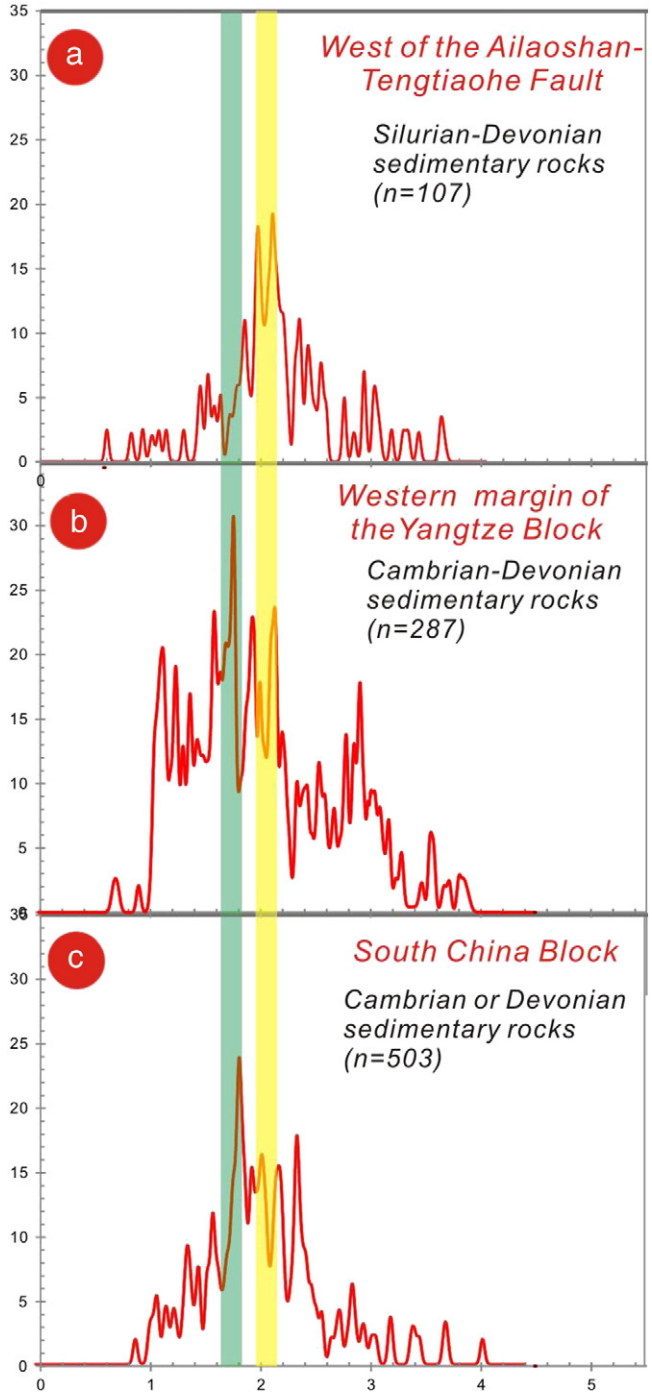

Fig. 11. Summary of detrital zircon Hf modal age T^{C}_{DM} distributions of sedimentary rocks of this study and previous works. (a) Compilation of the samples in this study from west of the Ailaoshan–Tengtiaohe fault. (b) Compilation of the samples in this study from the western margin of the Yangtze Block. (c) Compilation of detrital zircon Hf modal age T^{C}_{DM} for the Lower Paleozoic sequence from the South China Block (data source are from Duan et al. (2011) and Xu et al. (2013)). Important age peaks are shown in color bands.

U–Pb ages and Hf isotopes from the Laowangzhai–Mojiang suspect terrane (i.e., northern part of the Mojiang–Lvchun area defined in this study, Fig. 2), which located between the above two suggested sutures, display similar characteristics with those of the Indochina–Simao Block but different from that for the Yangtze block (Q.F. Wang et al., 2014). Therefore, the Laowangzhai–Mojiang suspect terrane is part of the Indochina–Simao block and the suture is unlikely to lie along Lixiangjiang fault. Q.F. Wang et al. (2014) proposed the Jiujia–Anding fault as the new suture zone in the northern part of the Mojiang–Lvchun area based on ophiolite occurrence. Nevertheless, ophiolites have not been discovered in the southern part of the Ailaoshan Belt. As there is no sedimentary detrital zircon data obtained from the area between the Jiujia–Anding fault and Ailaoshan fault, so we cannot exclude the possibility of the Ailaoshan fault to the boundary. More importantly, the exact location of the suture in the south of Mojiang remains uncertain due to lack of data for this region at present (Q.F. Wang et al., 2014).

In this study, we have analyzed more than 1000 detrital zircon grains from total 14 Cambrian–Devonian sedimentary samples across the whole Ailaoshan belt. These 14 samples covered all the terranes bounded by the three faults mentioned above. Therefore we can use them to test those previously suggested boundaries. Our Silurian–Devonian samples from the Mojiang (SM09-135, Fig. 2) and Lvchun area (CLX-57, CLX-63, YN-135 and K10-25B, Fig. 2) are likely to have received deritals from the Indochian-Simao Block and the northern East Gondwana. Therefore, the Silurian–Devonian sediments in Mojiang–Lvchun area were unlikely to be deposited on the passive margin of the western Yangtze Block as suggested by previous studies (Zhong et al., 1998; Wang et al., 2000), and the whole Mojiang–Lvchun area is not a part of the Yangtze Block but Simao Block. Thus it demonstrates that the Amojiang–Lixianjiang fault is unlikely to represent the suture zone.

In addition, the siliciclastics (YN-41 and YN-54) from the area between the Jiujia–Anding and Ailaoshan faults have the same detrital zircon populations (and thus provenance) with those of the sandstones from the rest of the Mojiang–Lvchun area west of the Jiujia–Anding fault, thus the Jiujia–Anding fault is excluded as a possible candidate for the suture.

Therefore, the Yangtze/Indochina–Simao suture is most likely to lie along the northern segment of the Ailaoshan fault. The southern continuation of the suture may lie along the Tengtiaohe fault instead of the southern segment of the Ailaoshan fault. This is not only because suspected ophiolites have been reported along the Tengtiaohe fault (Wang and Wang, 2004), but also because the Jinping area (west of the southern Ailaoshan fault segment) may have been connected to South China (Chung et al., 1997; Xiao et al., 2003; Wang et al., 2007).

5.3. The opening of the Ailaoshan Ocean

There are two main hypotheses about the opening of the Ailaoshan Ocean. The first one regards the Ailaoshan Ocean as a back-arc basin and had rifted and separated from the Yangtze Block in the Devonian-Permian in response to the northward subduction of the Main Paleo-Tethys (Wang et al., 2000; Metcalfe, 2006; Pan et al., 2012; Metcalfe, 2013); The second hypothesis advocates that the Ailaoshan Ocean was an Atlantic-type ocean basin and started its early continental rifting in the Early Devonian or the Silurian (Jian et al., 2009a,b; Lai, 2012).

The Paleozoic sequence in both the western Yangtze margin and Ailaoshan Belt was generally considered to be deposited on the western Yangtze continental shelf or slope (YNGMR, 1990; Xiong et al., 1998; Zhong et al., 1998; Wang et al., 2000). However, our results for these Silurian–Devonian Paleozoic sedimentary rocks demonstrate that the Ailaoshan (Mojiang–Lvchun area) and Yangtze have distinct sedimentary provenances since at least the Early Silurian. On the side of the Simao Block, samples show a highly consistent provenance from lower Silurian to lower Devonian, while a secular Silurian–Devonian change (more juvenile grains appeared in the relative young samples) can be visualized for the source of western margin samples of the Yangtze Block. Combined with siliciclastics from east and west of the Ailaoshan–Tengtiaohe fault have distinct source character, this discrepancy may indicate that there has existed a sea wide enough to separate the detrital source since at least the Early Silurian. Our Cambrian and Ordovician samples from the western Yangtze margin display a highly

matured, distal and tectonic stable source character, while the Middle Silurian to Lower Devonian samples have changed into an unmatured, proximal and tectonic relatively unstable source. A similar secular variation has also recorded in the samples from the Simao side (Table 1). It is worthy to note that one Lower Silurian sample (SM09-135) shows highly matured, distal and tectonic stable source character, another (YN-54) shows unmatured, proximal source character. Therefore, we conclude that the continental rifting may have started in the Early Silurian due to breakup of Gondwana. This conclusion is consistent with the presence of Panjiazhai Silurian alkaline continental rift basalts and possibly rift-related amphibolites in the Jinshajiang–Ailaoshan belts (Cheng and Shen, 1997; Jian et al., 2009a,b; Lai, 2012). The changes in sedimentary facies in Ailaoshan Belt (Fig. 3), from Silurian–Early Devonian siliciclastic rocks to Late Devonian–Carboniferous pelagic shale–limestone–chert (Xiong et al., 1998; Zhang and Lenz, 1998), suggest ongoing continental rifting and regional subsidence. This suggests that the opening time for the Ailaoshan Ocean is almost the same with that for the Main Paleo-Tethys (Silurian–Devonian) along the present Changning–Menglian–Inthanon suture (Metcalfe, 1996; Zhong et al., 1998; Feng, 2002; Metcalfe, 2006).

6. Conclusions

Based on our new detrital zircon U–Pb ages and Hf isotope data for the Cambrian to Upper Devonian sedimentary rocks from the western Yangtze margin and the Ailaoshan Belt, we conclude that:

1. Detrital zircons from the Cambrian to Upper Devonian western Yangtze sandstones contain a diagnostic age peak at 730–900 Ma. Detrital zircons of these peaks are characterized by both negative and positive $\varepsilon Hf(t)$ values. These characters suggest that the Yangtze Block was the main detrital source.
2. The Silurian–Devonian sandstones–siltstone samples from the Mojiang–Lvchun area of the Ailaoshan Belt display two distinctive detrital zircon age peaks at ca. 450 Ma and 950 Ma. Detrital zircons of ca. 450 Ma have generally negative $\varepsilon Hf(t)$ values. These characters indicate that the Indochina–Simao Block and the northern Gondwana were the detrital sources.
3. Detrital zircons from the Ailaoshan (Jinping area) siltstones display a major Neoproterozoic (730–900 Ma) cluster, similar to that of western Yangtze detrital zircons. Therefore, the Jinping area may have been part of or very close to the Yangtze Block. This conclusion is consistent with the occurrence of Late Permian, possibly ELIP-related, continental rift basalts in the Jinping area.
4. The Yangtze/Indochina–Simao suture may lie along or in close proximity to the Ailaoshan–Tengtiaohe fault.
5. Siliciclastic rocks from two sides of the Ailaoshan–Tengtiaohe suture have different provenances from at least the Early Silurian. This implies that the region may have developed a wide continental rift since the Early Silurian, which may have been further developed into a passive volcanic margin and ocean basin later in the Devonian–Carboniferous.

Supplementary data to this article can be found online at http://dx.doi.org/10.1016/j.gr.2015.08.006.

Acknowledgments

This study was financially supported by the National Natural Science Foundation of China (Project No. 41173007) and the Chinese Academy of Sciences (GIGCAS-135-Y234151001 and 100 Talents Program) to Dr. X.-P. XIA. This is a contribution IS 2129 to the Guangzhou Institute of Geochemistry, the Chinese Academy of Sciences.

References

Baker, J., Peate, D., Waight, T., Meyzen, C., 2004. Pb isotopic analysis of standards and samples using a 207Pb–204Pb double spike and thallium to correct for mass bias with a double-focusing MC–ICP–MS. Chemical Geology 211, 275–303.
Black, L.P., Gulson, B.L., 1978. The age of the mud tank carbonatite, Strangways Range, Northern Territory.
Black, L.P., Kamo, S.L., Allen, C.M., Aleinikoff, J.N., Davis, D.W., Korsch, R.J., Foudoulis, C., 2003. TEMORA 1: a new zircon standard for Phanerozoic U–Pb geochronology. Chemical Geology 200, 155–170.
Bouvier, A., Vervoort, J.D., Patchett, P.J., 2008. The Lu–Hf and Sm–Nd isotopic composition of CHUR: constraints from unequilibrated chondrites and implications for the bulk composition of terrestrial planets. Earth and Planetary Science Letters 273, 48–57.
Burrett, C., Zaw, K., Meffre, S., Lai, C.K., Khositanont, S., Chaodumrong, P., Udchachon, M., Ekins, S., Halpin, J., 2014. The configuration of Greater Gondwana—evidence from LA ICPMS, U–Pb geochronology of detrital zircons from the Palaeozoic and Mesozoic of Southeast Asia and China. Gondwana Research 26, 31–51.
Cai, Y., Wang, Y., Cawood, P.A., Fan, W., Liu, H., Xing, X., Zhang, Y., 2014. Neoproterozoic subduction along the Ailaoshan zone, South China: geochronological and geochemical evidence from amphibolite. Precambrian Research 245, 13–28.
Cawood, P.A., Wang, Y., Xu, Y., Zhao, G., 2013. Locating South China in Rodinia and Gondwana: a fragment of greater India lithosphere? Geology 41, 903–906.
Cheng, H.L., Shen, S.Y., 1997. Metamorphic basalts in Panjiazhai, Ailao Mountain area, Yunnan. Tethyan Geology 21, 62–72 (in Chinese with English abstract).
Chung, S.-L., Jahn, B.-m., 1995. Plume–lithosphere interaction in generation of the Emeishan flood basalts at the Permian–Triassic boundary. Geology 23, 889–892.
Chung, S.-L., Lee, T.-Y., Lo, C.-H., Wang, P.-L., Chen, C.-Y., Yem, N.T., Hoa, T.T., Genyao, W., 1997. Intraplate extension prior to continental extrusion along the Ailao Shan–Red River shear zone. Geology 25, 311–314.
Corfu, F., Hanchar, J.M., Hoskin, P.W., Kinny, P., 2003. Atlas of zircon textures. Reviews in Mineralogy and Geochemistry 53, 469–500.
Dong, Y., Liu, X., Santosh, M., Zhang, X., Chen, Q., Yang, C., Yang, Z., 2011. Neoproterozoic subduction tectonics of the northwestern Yangtze Block in South China: constrains from zircon U–Pb geochronology and geochemistry of mafic intrusions in the Hannan Massif. Precambrian Research 189, 66–90.
Dong, Y., Liu, X., Santosh, M., Chen, Q., Zhang, X., Li, W., He, D., Zhang, G., 2012. Neoproterozoic accretionary tectonics along the northwestern margin of the Yangtze Block, China: constraints from zircon U–Pb geochronology and geochemistry. Precambrian Research 196–197, 247–274.
Duan, L., Meng, Q.-R., Zhang, C.-L., Liu, X.-M., 2011. Tracing the position of the South China block in Gondwana: U–Pb ages and Hf isotopes of Devonian detrital zircons. Gondwana Research 19, 141–149.
Fan, W., Wang, Y., Zhang, A., Zhang, F., Zhang, Y., 2010. Permian arc–back-arc basin development along the Ailaoshan tectonic zone: geochemical, isotopic and geochronological evidence from the Mojiang volcanic rocks, Southwest China. Lithos 119, 553–568.
Faure, M., Lepvrier, C., Nguyen, V.V., Vu, T.V., Lin, W., Chen, Z., 2014. The South China block–Indochina collision: where, when, and how? Journal of Asian Earth Sciences 79, 260–274.
Feng, Q.-L., 2002. Stratigraphy of volcanic rocks in the Changning–Menglian Belt in southwestern Yunnan, China. Journal of Asian Earth Sciences 20, 657–664.
Findlay, R., 1997. The Song Ma Anticlinorium, northern Vietnam: the structure of an allochthonous terrane containing an early Palaeozoic island arc sequence. Journal of Asian Earth Sciences 15, 453–464.
Greentree, M.R., Li, Z.-X., 2008. The oldest known rocks in south–western China: SHRIMP U–Pb magmatic crystallisation age and detrital provenance analysis of the Paleoproterozoic Dahongshan Group. Journal of Asian Earth Sciences 33, 289–302.
Greentree, M.R., Li, Z.-X., Li, X.-H., Wu, H., 2006. Late Mesoproterozoic to earliest Neoproterozoic basin record of the Sibao orogenesis in western South China and relationship to the assembly of Rodinia. Precambrian Research 151, 79–100.
Griffin, W., Pearson, N., Belousova, E., Jackson, S., Van Achterbergh, E., O'Reilly, S.Y., Shee, S., 2000. The Hf isotope composition of cratonic mantle: LAM–MC–ICPMS analysis of zircon megacrysts in kimberlites. Geochimica et Cosmochimica Acta 64, 133–147.
Griffin, W., Wang, X., Jackson, S., Pearson, N., O'Reilly, S.Y., Xu, X., Zhou, X., 2002. Zircon chemistry and magma mixing, SE China: in-situ analysis of Hf isotopes, Tonglu and Pingtan igneous complexes. Lithos 61, 237–269.
Hara, H., Kunii, M., Hisada, K.-i., Ueno, K., Kamata, Y., Srichan, W., Charusiri, P., Charoentitirat, T., Watarai, M., Adachi, Y., Kurihara, T., 2012. Petrography and geochemistry of clastic rocks within the Inthanon zone, northern Thailand: implications for Paleo-Tethys subduction and convergence. Journal of Asian Earth Sciences 61, 2–15.
Huang, X.-L., Xu, Y.-G., Li, X.-H., Li, W.-X., Lan, J.-B., Zhang, H.-H., Liu, Y.-S., Wang, Y.-B., Li, H.-Y., Luo, Z.-Y., Yang, Q.-J., 2008. Petrogenesis and tectonic implications of Neoproterozoic, highly fractionated A-type granites from Mianning, South China. Precambrian Research 165, 190–204.
Jackson, S.E., Pearson, N.J., Griffin, W.L., Belousova, E.A., 2004. The application of laser ablation-inductively coupled plasma–mass spectrometry to in situ U–Pb zircon geochronology. Chemical Geology 211, 47–69.
Jian, P., Zhong, D.L., 2002. U–Pb zricon dating of the Caledonian Gongbo gabbro from the Mid-Jinshajiang area, Sichuan Province. Geological Review 48, 17–21 (in Chinese with English abstract).
Jian, P., Liu, D., Kröner, A., Zhang, Q., Wang, Y., Sun, X., Zhang, W., 2009a. Devonian to Permian plate tectonic cycle of the Paleo-Tethys Orogen in southwest China (I): geochemistry of ophiolites, arc/back-arc assemblages and within-plate igneous rocks. Lithos 113, 748–766.

Jian, P., Liu, D., Kröner, A., Zhang, Q., Wang, Y., Sun, X., Zhang, W., 2009b. Devonian to Permian plate tectonic cycle of the Paleo-Tethys Orogen in southwest China (II): insights from zircon ages of ophiolites, arc/back-arc assemblages and within-plate igneous rocks and generation of the Emeishan CFB province. Lithos 113, 767–784.
Kamata, Y., Maezawa, A., Hara, H., Ueno, K., Hisada, K.-i., Sardsud, A., Charoentitirat, T., Charusiri, P., 2012. Basaltic activity preserved in an Upper Permian radiolarian chert from the Paleo-Tethys in the Inthanon Zone, northern Thailand. Journal of Asian Earth Sciences 61, 51–61.
Khositanont, S., Panjasawatwong, Y., Ounchanum, P., Thanasuthipitak, T., Zaw, K., Meffre, S., 2008. Petrochemistry and zircon age determination of Loei–Phetchabun volcanic rocks. Proceedings of the International Symposia on Geoscience Resources and Environments of Asian Terranes (GREAT 2008), pp. 272–278.
Lai, C.K., 2012. Tectonic evolution of the Ailaoshan fold belt in SW Yunnan, China, ARC Center of Excellence in Ore Deposits (CODES). ARC Center of Excellence in Ore Deposits (CODES). University of Tasmania, Hobart.
Lai, C.K., Meffre, S., Crawford, A.J., Zaw, K., Halpin, J.A., Xue, C.D., Salam, A., 2014a. The Central Ailaoshan ophiolite and modern analogs. Gondwana Research 26, 75–88.
Lai, C.K., Meffre, S., Crawford, A.J., Zaw, K., Xue, C.D., Halpin, J.A., 2014b. The Western Ailaoshan Volcanic Belts and their SE Asia connection: a new tectonic model for the Eastern Indochina Block. Gondwana Research 26, 52–74.
Lehmann, B., Zhao, X., Zhou, M., Du, A., Mao, J., Zeng, P., Henjes-Kunst, F., Heppe, K., 2013. Mid-Silurian back-arc spreading at the northeastern margin of Gondwana: the Dapingzhang dacite-hosted massive sulfide deposit, Lancangjiang zone, southwestern Yunnan, China. Gondwana Research 24, 648–663.
Leloup, P.H., Lacassin, R., Tapponnier, P., Schärer, U., Zhong, D., Liu, X., Zhang, L., Ji, S., Trinh, P.T., 1995. The Ailao Shan–Red River shear zone (Yunnan, China), Tertiary transform boundary of Indochina. Tectonophysics 251, 3–84.
Leloup, P., Tapponnier, P., Lacassin, R., Searle, M., 2007. Discussion on the role of the Red River shear zone, Yunnan and Vietnam, in the continental extrusion of SE Asia Journal, Vol. 163, 2006, 1025–1036. Journal of the Geological Society 164, 1253–1260.
Lepvrier, C., Van Vuong, N., Maluski, H., Truong Thi, P., Van Vu, T., 2008. Indosinian tectonics in Vietnam. Comptes Rendus Geoscience 340, 94–111.
Li, X., 2003. Neoproterozoic granitoids in South China: crustal melting above a mantle plume at ca. 825 Ma? Precambrian Research 122, 45–83.
Li, Z., 2003. Geochronology of Neoproterozoic syn-rift magmatism in the Yangtze Craton, South China and correlations with other continents: evidence for a mantle superplume that broke up Rodinia. Precambrian Research 122, 85–109.
Li, X.-h., Li, Z.-X., Zhou, H., Liu, Y., Kinny, P.D., 2002. U–Pb zircon geochronology, geochemistry and Nd isotopic study of Neoproterozoic bimodal volcanic rocks in the Kangdian Rift of South China: implications for the initial rifting of Rodinia. Precambrian Research 113, 135–154.
Li, X.H., Long, W.G., Li, Q.L., Liu, Y., Zheng, Y.F., Yang, Y.H., Chamberlain, K.R., Wan, D.F., Guo, C.H., Wang, X.C., 2010. Penglai zircon megacrysts: a potential new working reference material for microbeam determination of Hf–O isotopes and U–Pb age. Geostandards and Geoanalytical Research 34, 117–134.
Lin, T.-H., Chung, S.-L., Chiu, H.-Y., Wu, F.-Y., Yeh, M.-W., Searle, M.P., Iizuka, Y., 2012. Zircon U–Pb and Hf isotope constraints from the Ailao Shan–Red River shear zone on the tectonic and crustal evolution of southwestern China. Chemical Geology 291, 23–37.
Liu, J., Wang, A., Cao, S., Zou, Y., Tang, Y., Chen, Y., 2008. Geochronology and tectonic implication of migmatites from Diancangshan, Western Ynnnan, China. Acta Petrologica Sinica 24, 413–420 (in Chinese with English abstract).
Ludwig, K.R.L., 2003. Isoplot 3.0. A Geochronological Toolkit for Microsoft Excel. Berkeley Geochron, Center Spec.
Mao, X., Wang, L., Li, B., Wang, B., Wang, D., Yin, F., Sun, Z., 2012. Discovery of the Late Silurian volcanic rocks in the Dazhonghe area, Yunxian-Jinggu volcanic arc belt, western Yunnan, China and its geological significance. Acta Petrologica Sinica 28, 1517–1528 (in Chinese with English abstract).
Metcalfe, I., 1996. Gondwanaland dispersion, Asian accretion and evolution of eastern Tethys*. Australian Journal of Earth Sciences 43, 605–623.
Metcalfe, I., 2002. Permian tectonic framework and palaeogeography of SE Asia. Journal of Asian Earth Sciences 20, 551–566.
Metcalfe, I., 2006. Palaeozoic and Mesozoic tectonic evolution and palaeogeography of East Asian crustal fragments: the Korean Peninsula in context. Gondwana Research 9, 24–46.
Metcalfe, I., 2011. Palaeozoic–Mesozoic history of SE Asia. Geological Society, London, Special Publications 355, 7–35.
Metcalfe, I., 2013. Gondwana dispersion and Asian accretion: tectonic and palaeogeographic evolution of eastern Tethys. Journal of Asian Earth Sciences 66, 1–33.
Mo, X., Shen, S., Zhu, Q., 1998. Volcanics, ophiolite and mineralization of middle-southern part in Sanjiang area of southwest China. Geological Press, Beijing.
Nagy, E.A., Maluski, H., Lepvrier, C., Schärer, U., Thi, P.T., Leyreloup, A., Van Thich, V., 2001. Geodynamic Significance of the Kontum Massif in Central Vietnam: composite 40Ar/39Ar and U–Pb Ages from Paleozoic to Triassic. The Journal of Geology 109, 755–770.
Nie, X., Feng, Q., Qian, X., Wang, Y., 2015. Magmatic record of Prototethyan evolution in SW Yunnan, China: geochemical, zircon U–Pb geochronological and Lu–Hf isotopic evidence from the Huimin metavolcanic rocks in the southern Lancangjiang zone. Gondwana Research 28, 757–768.
Pan, G.T., X.Q., Hou, Z.Q., 2003. Archipelagic Orogenesis, Metallogenic Systems and Assessment of the Mineral Resources along the Nujiang–Langcangjiang–Jinshajiang Area in South western China. Geological Publishing House, Beijing.
Pan, G., Wang, L., Li, R., Yuan, S., Ji, W., Yin, F., Zhang, W., Wang, B., 2012. Tectonic evolution of the Qinghai–Tibet Plateau. Journal of Asian Earth Sciences 53, 3–14.
Pei, X., Li, Z., Ding, S., Li, R., Feng, J., Sun, Y., Zhang, Y., Liu, Z., 2009. Neoproterozoic Jiaoziding peraluminous granite in the northwestern margin of Yangtze Block: zircon SHRIMP U–Pb age and geochemistry and their tectonic significance. Earth Science Frontiers 16, 231–249 (in Chinese with English abstract).
Qi, X., Zeng, L., Zhu, L., Hu, Z., Hou, K., 2012. Zircon U–Pb and Lu–Hf isotopic systematics of the Daping plutonic rocks: implications for the Neoproterozoic tectonic evolution of the northeastern margin of the Indochina block, Southwest China. Gondwana Research 21, 180–193.
Qi, X., Santosh, M., Zhu, L., Zhao, Y., Hu, Z., Zhang, C., Ji, F., 2014. Mid-Neoproterozoic arc magmatism in the northeastern margin of the Indochina block, SW China: geochronological and petrogenetic constraints and implications for Gondwana assembly. Precambrian Research 245, 207–224.
Qiu, Y.M., Gao, S., McNaughton, N.J., Groves, D.I., Ling, W., 2000. First evidence of >3.2 Ga continental crust in the Yangtze craton of south China and its implications for Archean crustal evolution and Phanerozoic tectonics. Geology 28, 11–14.
Rogers, J.J.W., Santosh, M., 2003. Supercontinents in Earth History. Gondwana Research 6, 357–368.
Scherer, E., Munker, C., Mezger, K., 2001. Calibration of the lutetium–hafnium clock. Science 293, 683–687.
Searle, M.P., Yeh, M.W., Lin, T.H., Chung, S.L., 2010. Structural constraints on the timing of left-lateral shear along the Red River shear zone in the Ailao Shan and Diancang Shan Ranges, Yunnan, SW China. Geosphere 6, 316–338.
Shellnutt, J.G., Zhou, M.-F., 2007. Permian peralkaline, peraluminous and metaluminous A-type granites in the Panxi district, SW China: their relationship to the Emeishan mantle plume. Chemical Geology 243, 286–316.
Shellnutt, J.G., Zhou, M.-F., Yan, D.-P., Wang, Y., 2008. Longevity of the Permian Emeishan mantle plume (SW China): 1 ma, 8 Ma or 18 Ma? Geological Magazine 145, 373–388.
Sláma, J., Košler, J., Condon, D.J., Crowley, J.L., Gerdes, A., Hanchar, J.M., Horstwood, M.S.A., Morris, G.A., Nasdala, L., Norberg, N., Schaltegger, U., Schoene, B., Tubrett, M.N., Whitehouse, M.J., 2008. Plešovice zircon — a new natural reference material for U–Pb and Hf isotopic microanalysis. Chemical Geology 249, 1–35.
Sone, M., Metcalfe, I., 2008. Parallel Tethyan sutures in mainland Southeast Asia: new insights for Palaeo-Tethys closure and implications for the Indosinian orogeny. Comptes Rendus Geoscience 340, 166–179.
Sun, W., Zhou, M., Yan, D., Li, J., Ma, Y., 2008. Provenance and tectonic setting of the Neoproterozoic Yanbian Group, western Yangtze Block (SW China). Precambrian Research 167, 213–236.
Sun, W.-H., Zhou, M.-F., Gao, J.-F., Yang, Y.-H., Zhao, X.-F., Zhao, J.-H., 2009. Detrital zircon U–Pb geochronological and Lu–Hf isotopic constraints on the Precambrian magmatic and crustal evolution of the western Yangtze Block, SW China. Precambrian Research 172, 99–126.
Tapponnier, P., Lacassin, R., Leloup, P.H., Scharer, U., Zhong, D.L., Wu, H.W., Liu, X.H., Ji, S.C., Zhang, L.S., Zhong, J.Y., 1990. The Ailao Shan Red River metamorphic belt — tertiary left-lateral shear between Indochina and South China. Nature 343, 431–437.
Tran, T., Nguyen, V., 2006. Tectonic setting of intrusive complexes in an area adjacent to Muong Lay Town, Dien Bien Province. Science and Technology. Journal of Mining and Geology 14, 43–52.
Tran, H.T., Zaw, K., Halpin, J.A., Manaka, T., Meffre, S., Lai, C.-K., Lee, Y., Le, H.V., Dinh, S., 2014. The Tam Ky-Phuoc Son Shear Zone in central Vietnam: tectonic and metallogenic implications. Gondwana Research 26, 144–164.
Usuki, T., Lan, C.-Y., Wang, K.-L., Chiu, H.-Y., 2013. Linking the Indochina block and Gondwana during the Early Paleozoic: evidence from U–Pb ages and Hf isotopes of detrital zircons. Tectonophysics 586, 145–159.
Vervoort, J.D., Patchett, P.J., Söderlund, U., Baker, M., 2004. Isotopic composition of Yb and the determination of Lu concentrations and Lu/Hf ratios by isotope dilution using MC–ICPMS. Geochemistry, Geophysics, Geosystems 5, Q11002.
Wang, S.H., Wang, Z.B., 2004. The discovery of structural melange–ophiolite belt in the south section of Ailaoshan orogenic. Yunnan Geology 23, 287–303 (in Chinese with English abstract).
Wang, X., Metcalfe, I., Jian, P., He, L., Wang, C., 2000. The Jinshajiang–Ailaoshan suture zone, China: tectonostratigraphy, age and evolution. Journal of Asian Earth Sciences 18, 675–690.
Wang, C.Y., Zhou, M.-F., Qi, L., 2007. Permian flood basalts and mafic intrusions in the Jinping (SW China)–Song Da (northern Vietnam) district: mantle sources, crustal contamination and sulfide segregation. Chemical Geology 243, 317–343.
Wang, X.-C., Li, X.-H., Li, W.-X., Li, Z.-X., Liu, Y., Yang, Y.-H., Liang, X.-R., Tu, X.-L., 2008. The Bikou basalts in the northwestern Yangtze block, South China: remnants of 820–810 Ma continental flood basalts? Geological Society of America Bulletin 120, 1478–1492.
Wang, P.-L., Lo, C.-H., Lan, C.-Y., Chung, S.-L., Lee, T.-Y., Nam, T.N., Sano, Y., 2011. Thermochronology of the PoSen complex, northern Vietnam: implications for tectonic evolution in SE Asia. Journal of Asian Earth Sciences 40, 1044–1055.
Wang, L.-J., Yu, J.-H., Griffin, W.L., O'Reilly, S.Y., 2012. Early crustal evolution in the western Yangtze Block: evidence from U–Pb and Lu–Hf isotopes on detrital zircons from sedimentary rocks. Precambrian Research 222–223, 368–385.
Wang, B.D., Wang, L.Q., Pan, G.T., Yin, F.G., Wang, D.B., Tang, Y., 2013. U–Pb zircon dating of Early Paleozoic gabbro from the Nantinghe ophiolite in the Changning–Menglian suture zone and its geological implication. Chinese Science Bulletin 58, 344–354 (in Chinese with English abstract).
Wang, Y., Zhang, A., Fan, W., Zhang, Y., Zhang, Y., 2013. Origin of paleosubduction-modified mantle for Silurian gabbro in the Cathaysia Block: geochronological and geochemical evidence. Lithos 160, 37–54.
Wang, L., Liu, C., Gao, X., Zhang, H., 2014a. Provenance and paleogeography of the Late Cretaceous Mengyejing Formation, Simao Basin, southeastern Tibetan Plateau: whole-rock geochemistry, U–Pb geochronology, and Hf isotopic constraints. Sedimentary Geology 304, 44–58.

Wang, Q.F., Deng, J., Li, C.S., Li, G.J., Yu, L., Qiao, L., 2014. The boundary between the Simao and Yangtze blocks and their locations in Gondwana and Rodinia: constraints from detrital and inherited zircons. Gondwana Research 26, 438–448.
Wiedenbeck, M., Alle, P., Corfu, F., Griffin, W., Meier, M., Oberli, F., Quadt, A.v., Roddick, J., Spiegel, W., 1995. Three natural zircon standards for U–Th–Pb, Lu–Hf, trace element and REE analyses. Geostandards Newsletter 19, 1–23.
Wu, H., Boulter, C.A., Ke, B., Stow, D.A.V., Wang, Z., 1995. The Changning–Menglian suture zone; a segment of the major Cathaysian–Gondwana divide in Southeast Asia. Tectonophysics 242, 267–280.
Xia, X.P., Ren, Z.Y., Wei, G.J., Zhang, L., Sun, M., Wang, Y.J., 2013. In situ rutile U–Pb dating by laser ablation–MC–ICPMS. Geochemical Journal 47, 459–468.
Xiao, L., Xu, Y.-G., Chung, S.-L., He, B., Mei, H., 2003. Chemostratigraphic Correlation of Upper Permian Lavas from Yunnan Province, China: extent of the Emeishan Large Igneous Province. International Geology Review 45, 753–766.
Xiong, J.Y., Zhang, Z.B.,Cai, L.S.,Hu, J.J.,Zhang, W.M., 1998. Study on the method of the 1: 50000 regional geological mapping in continental orogenic belt: an example of Ailaoshan orogenic belt (in Chinese with English abstract). China University of Geosciences Press Wuhan.
Xu, Y.-G., Luo, Z.-Y., Huang, X.-L., He, B., Xiao, L., Xie, L.-W., Shi, Y.-R., 2008. Zircon U–Pb and Hf isotope constraints on crustal melting associated with the Emeishan mantle plume. Geochimica et Cosmochimica Acta 72, 3084–3104.
Xu, Y., Cawood, P.A., Du, Y., Hu, L., Yu, W., Zhu, Y., Li, W., 2013. Linking south China to northern Australia and India on the margin of Gondwana: constraints from detrital zircon U–Pb and Hf isotopes in Cambrian strata. Tectonics 32, 1547–1558.
Yan, Q., Hanson, A.D., Wang, Z., Druschke, P.A., Yan, Z., Wang, T., Liu, D., Song, B., Jian, P., Zhou, H., 2004. Neoproterozoic subduction and rifting on the northern margin of the Yangtze Plate, China: implications for Rodinia reconstruction. International Geology Review 46, 817–832.
YNGMR, 1990. Regional Geology of Yunnan Province. Geological Publishing House, Beijing.
Zaw, Meffre, S., Lai, C.-K., Burrett, C., Santosh, M., Graham, I., Manaka, T., Salam, A., Kamvong, T., Cromie, P., 2014. Tectonics and metallogeny of mainland Southeast Asia — a review and contribution. Gondwana Research 26, 5–30.
Zhang, Y.-D., Lenz, A.C., 1998. Early Devonian graptolites from Southwest Yunnan, China. Journal of Paleontology 353–360.
Zhao, G., Cawood, P.A., 2012. Precambrian geology of China. Precambrian Research 222–223, 13–54.
Zhao, J.-H., Zhou, M.-F., 2007. Geochemistry of Neoproterozoic mafic intrusions in the Panzhihua district (Sichuan Province, SW China): implications for subduction-related metasomatism in the upper mantle. Precambrian Research 152, 27–47.
Zhao, J.-H., Zhou, M.-F., 2008. Neoproterozoic adakitic plutons in the northern margin of the Yangtze Block, China: partial melting of a thickened lower crust and implications for secular crustal evolution. Lithos 104, 231–248.
Zhao, J.-H., Zhou, M.-F., 2009. Secular evolution of the Neoproterozoic lithospheric mantle underneath the northern margin of the Yangtze Block, South China. Lithos 107, 152–168.
Zhao, X., Zhou, M., Li, J., Wu, F., 2008. Association of Neoproterozoic A- and I-type granites in South China: implications for generation of A-type granites in a subduction-related environment. Chemical Geology 257, 1–15.
Zhao, J.-H., Zhou, M.-F., Zheng, J.-P., Fang, S.-M., 2010. Neoproterozoic crustal growth and reworking of the Northwestern Yangtze Block: constraints from the Xixiang dioritic intrusion, South China. Lithos 120, 439–452.
Zhao, J.-H., Zhou, M.-F., Zheng, J.-P., 2013. Neoproterozoic high-K granites produced by melting of newly formed mafic crust in the Huangling region, South China. Precambrian Research 233, 93–107.
Zhong, D.L., Chong, P.L., Zhai, M.G., Zhang, C.H., Chen, T.E., 1998. Paleotethyan orogeny in the western Yunnan and Sichuan (in Chinese with English abstract). Science Publishing House, Beijing.
Zhou, M.-F., Yan, D.-P., Kennedy, A.K., Li, Y., Ding, J., 2002a. SHRIMP U–Pb zircon geochronological and geochemical evidence for Neoproterozoic arc-magmatism along the western margin of the Yangtze Block, South China. Earth and Planetary Science Letters 196, 51–67.
Zhou, M.F., Kennedy, A.K., Sun, M., Malpas, J., Lesher, C.M., 2002b. Neoproterozoic arc-related mafic intrusions along the northern margin of South China: implications for the accretion of Rodinia. The Journal of Geology 110, 611–618.
Zhou, M., Ma, Y., Yan, D., Xia, X., Zhao, J., Sun, M., 2006. The Yanbian Terrane (Southern Sichuan Province, SW China): a Neoproterozoic arc assemblage in the western margin of the Yangtze Block. Precambrian Research 144, 19–38.
Zhou, Y., Liang, X., Liang, X., Jiang, Y., Wang, C., Fu, J., Shao, T., 2015. U–Pb geochronology and Hf-isotopes on detrital zircons of Lower Paleozoic strata from Hainan Island: new clues for the early crustal evolution of southeastern South China. Gondwana Research 27, 1586–1598.
Zhu, W.G., Zhong, H., Deng, H.L., Wilson, A.H., Liu, B.G., Li, C.Y., Qin, Y., 2006. SHRIMP Zircon U–Pb Age, Geochemistry, and Nd-Sr Isotopes of the Gaojiacun Mafic–Ultramafic Intrusive Complex, Southwest China. International Geology Review 48, 650–668.
Zhu, W.-G., Zhong, H., Li, X.-H., Deng, H.-L., He, D.-F., Wu, K.-W., Bai, Z.-J., 2008. SHRIMP zircon U–Pb geochronology, elemental, and Nd isotopic geochemistry of the Neoproterozoic mafic dykes in the Yanbian area, SW China. Precambrian Research 164, 66–85.
Zi, J.-W., Cawood, P.A., Fan, W.-M., Wang, Y.-J., Tohver, E., 2012. Contrasting rift and subduction-related plagiogranites in the Jinshajiang ophiolitic mélange, southwest China, and implications for the Paleo-Tethys. Tectonics 31 (n/a-n/a).
Zi, J.W., Cawood, P.A., Fan, W.M., Tohver, E., Wang, Y.J., McCuaig, T.C., Peng, T.P., 2013. Late Permian–Triassic magmatic evolution in the Jinshajiang orogenic belt, SW China and implications for orogenic processes following closure of the Paleo-Tethys. American Journal of Science 313, 81–112.